

DIFFERENTIAL NEUROGENESIS IN THE ADULT RAT DENTATE GYRUS

NEAL MELVIN

M.Sc., University of Calgary, 2001
B.Sc., University of Lethbridge, 1998

A Thesis

Submitted to the Graduate Council
of the University of Lethbridge
in Partial Fulfilment of the
Requirements for the Degree

DOCTOR OF PHILOSOPHY

Department of Neuroscience
University of Lethbridge
LETHBRIDGE, ALBERTA, CANADA

© Neal R. Melvin, 2008

Dedication

This thesis is dedicated to the memory of my mother, June Sharon Melvin, who passed away on January 17, 1998. I know that you would have loved to be a part of this. It never gets easier, it only gets less frequent. I love you mom.

Abstract

Adult neurogenesis is a fundamental feature of mammalian nervous systems. Curiously, neurogenesis in the dentate gyrus is typically regarded as homogenous. This thesis challenges that view, and reports the discovery and characterization of a novel region of the dentate gyrus that consistently lacks basal neurogenesis. We demonstrate that this area, referred to as the neurogenically quiescent zone, represents approximately 1.5% of the total volume of the dentate gyrus, and that its location is invariant among animals. This region contains several critical cell types and molecular factors that are known to be critical to the neurogenic niche, including stem cells. We also present data that attempt to conceptualize the existence of this region in the context of early age-related declines in neurogenesis. Finally, we demonstrate that, under some behavioural conditions, neurogenesis can be induced in this region, suggesting that, under basal conditions, it may simply lack the presence of pro-neurogenic factors.

Acknowledgements

It would not be possible to complete a work of this magnitude without the influence of a wide variety of people. To begin with, I would like to thank Dr. Robert Sutherland for his extreme generosity and excellent tutelage. Thank you for the high degree of independence you let me have right from the beginning, and for being open to me introducing new concepts and methods to your lab. I would also like to thank Drs. Glen Prusky and Richard Dyck, for giving me the opportunities in my career that I didn't always realise I needed.

I would also like to formally acknowledge the members of my committee, Drs. James Thomas and Gerlinde Metz, for your excellent feedback on my work, and to Dr. Brian Christie for agreeing to serve as my external examiner. Thanks to Drs. Lutz Slomianka, Daniel Peterson, and Luis Cruz-Orive for your advice on experimental design and stereological analyses, and Drs. Amelia Eisch, Nicole Sherren, Marie Monfils, Geniva Liu, Hugo Lehmann, and Alex Klein for your support and stimulating discussions about science. To Drs. Petra Hermann and Wic Wildering, I've learned as much about science from you both as from anyone. To Naomi Cramer, if there was an annual award for the Most Valuable Player of the CCBN, you'd have my vote every year.

Thanks to all members of the Sutherland lab, past and present, who have given the working atmosphere a great balance of intellectual intensity and comic relief. I would also like to acknowledge Keri Colwell for her friendship, and willingness to help me both in and out of the lab and Doug Bray, for being a very accommodating and an invaluable resource. Thanks for all of your advice through the years.

The University of Lethbridge affords a relatively unique opportunity to interact with a large number of very talented undergraduate students, and several deserve my personal thanks. To David Chatterton, Amanda Shmyrko, and Jerrah Sawatsky, I appreciate your help in the lab. You are all very bright, and I know you'll go on to make great contributions in your chosen fields. Thanks also to all the students in my Neuroscience 3600 and 3625 classes, who never let me forget how much I love teaching.

Several friends helped me survive the final stages of this process, and said all the right things at the right times. Vinay Bharadia, you have been my best friend for 8 years now, and you have always given me excellent advice and been willing to go out of your way to be one of the most supportive people I've ever known. Daniel Poda, you have been a great friend to me, and I have learned a lot from you. I wish most of my sentences to you didn't start with "Can you give me a hand with something?". To Nichole Goodyear, Shane Ferguson, Val Beaman, Rachel Bennett, Gillian Grossman, Sara Berenguer, Jennifer Dawson, Wayne Tschetter, Shannon Patrick, Shawna Williams, Tara Giacobbo, Freya Zaltz, Catherine Marshall, and Natalya Nicholson, thank you for your personal support at various times during my time in Lethbridge. You have each made fundamental contributions to my life.

Three people deserve special acknowledgement. To Chrissie Szekely, thank you for sharing your life with me. You will always be one of the most important people in my life. To Grace Szekely, I know you are just learning to read now, but I hope you will read this someday. You are an amazing little girl, and I will never be able to express how much I love you. Even though you're only 5 years old, you have had a very powerful influence on me, and I'm glad I got to see you grow up. You are your mom's daughter in

every single way. Lastly, I would like to thank my girlfriend, Julia Townell. You have done more for me than anyone else ever has, and I love you for it. Thank you for tolerating me when I was acting like a scientist.

TABLE OF CONTENTS

APPROVAL PAGE	p. ii
DEDICATION PAGE	p. iii
ABSTRACT	p. iv
ACKNOWLEDGEMENTS	p. v
TABLE OF CONTENTS	p. viii
LIST OF TABLES	p. xii
LIST OF FIGURES	p. xiii
ABBREVIATIONS	p. xv
CHAPTER ONE	
Overview	p. 1
Identifying Neurogenesis-Related Cellular Phenotypes	p. 2
Neurogenesis in its Cellular Context: The Neurogenic Niche	p. 7
A Myriad of Factors Modulate Neurogenesis	p. 11
Growth Factors and Neurogenesis	p. 12
Behavioural Experience can Modulate Neurogenesis	p. 14
Neurogenesis and Ageing	p. 16
Identifying the Molecular Mechanisms Mediating Basal Neurogenesis in the Adult DG	p. 18
CHAPTER TWO	
The HPC and DG Neurogenic Heterogeneity	p. 21
Materials and Methods	p. 24
Animals	p. 24
Perfusions	p. 24

Histology	p. 24
Antibodies	p. 25
BrdU Administration	p. 25
Immunohistochemistry	p. 25
Quantification of BrdU and Ki-67+ Cells	p. 29
Epi-fluorescence Microscopy, Confocal Microscopy, and Image Analysis	p. 29
Cavalieri Volume Estimates	p. 30
Three Dimensional (3D) Modelling	p. 32
Results	p. 32
The Size and Location of the NQZ	p. 32
The NQZ in 3 Dimensions	p. 33
The Anatomical Size and Location of the NQZ is Consistent Between Animals	p. 36
Stereological Design and Sampling Error Prediction	p. 36
The NQZ is Consistently Devoid of Cell Proliferation	p. 49
The NQZ Contains Similar Cell Types to Other Areas of the DG	p. 53
The NQZ Contains Stem Cells	p. 55
The NQZ Contains a Vascular Network	p. 58
Discussion	p. 62
CHAPTER THREE	
DG Development, Ageing, and Neurogenesis	p. 64
Materials and Methods	p. 68

Animals	p. 68
Perfusions	p. 68
Histology	p. 69
Antibodies	p. 69
Immunohistochemistry	p. 69
Cavalieri Volume Estimates	p. 69
Co-localisation of FGF-2 in SGZ Astrocytes	p. 70
Results	p. 71
The NQZ Volume Fraction Increases with Age	p. 71
FGF-2 Expression in the NQZ is Qualitatively Similar to non-NQZ Regions	p. 75
All GFAP+ Astrocytes in the NQZ and non-NQZ Express FGF-2	p. 75
Discussion	p. 78
CHAPTER FOUR	
Neurogenesis can be Behaviourally Induced in the DG	p. 86
Materials and Methods	p. 87
Animals	p. 87
Short-term Wheel Running	p. 87
Longer-term Wheel Running	p. 88
Alternating Wheel Running and Environmental Enrichment	p. 88
Perfusions	p. 89
Histology	p. 89

Immunohistochemistry and Imaging	p. 89
Results	p. 89
Wheel Running Alone may not Induce NQZ Neurogenesis	p. 89
NQZ Neurogenesis can be Induced Under Some Conditions	p. 93
Discussion	p. 93
CHAPTER FIVE	
Potential Reasons for the Existence of the NQZ	p. 99
The Utility of the NQZ	p. 101
REFERENCES	p. 107

LIST OF TABLES

Table 1.	Key characteristics of the major cell types involved in neurogenesis.	p. 9
Table 2.	Antibodies, dilutions, and suppliers used in immunohistochemical experiments.	p. 26
Table 3.	A sample volume estimate and CE calculation from animal #98.	p. 44
Table 4.	Quantitative estimates of the volume of the granule cell layer (GCL), the neurogenically quiescent zone (NQZ), the NQZ volume fraction, and estimates of precision.	p. 46
Table 5.	Quantitative estimates of the volume of the granule cell layer (GCL), the neurogenically quiescent zone (NQZ), the NQZ volume fraction, and estimates of precision across age.	p. 74

LIST OF FIGURES

Figure 1.	The DG is a site of adult neurogenesis.	p. 8
Figure 2.	The general organization of the HPC as seen in the coronal plane.	p. 22
Figure 3.	The anatomical location of the NQZ.	p. 34
Figure 4.	A 3D reconstruction of the NQZ.	p. 35
Figure 5.	The neurogenically quiescent zone (NQZ) is similar in size and position across animals.	p. 37
Figure 6.	NQZ lacks cellular proliferation as assessed by bromodeoxyuridine (BrdU).	p. 51
Figure 7.	No Ki-67+ cycling cells were observed in the NQZ.	p. 52
Figure 8.	The distribution of mature neurons and glial cells is qualitatively similar in the NQZ versus non-NQZ areas.	p. 54
Figure 9.	Granule neurons in the GCL of the NQZ have a typical dendritic morphology.	p. 56
Figure 10.	The SGZ of the NQZ contains stem cells.	p. 57
Figure 11.	The SGZ of the NQZ contains stem cells.	p. 59
Figure 12.	The NQZ contains vasculature.	p. 60
Figure 13.	The density of blood vessels in the NQZ is similar to non-NQZ areas of the DG.	p. 61
Figure 14.	The NQZ is age-dependent.	p. 73
Figure 15.	The NQZ expands across age.	p. 76

Figure 16.	The density of FGF-2 expressing cells is similar in NQZ and non-NQZ regions of the adult DG.	p. 77
Figure 17.	Complete co-expression of FGF-2 in SGZ astrocytes.	p. 79
Figure 18.	Distance ran per day in short-term runners.	p. 91
Figure 19.	Distance ran per day in longer-term runners.	p. 92
Figure 20.	Alternating exposure to wheel running and environmental enrichment induces neurogenesis in the NQZ.	p. 94

ABBREVIATIONS

3D	Three dimensional
ANOVA	Analysis of variance
BrdU	Bromodeoxyuridine
CE	Coefficient of error
DCX	Doublecortin
DG	Dentate gyrus
FGF-2	Fibroblast growth factor 2
GABA	Gamma amino butyric acid
GCL	Granule cell layer
GFAP	Glial fibrillary acidic protein
GFP	Green fluorescence protein
HPC	Hippocampus
IGF-I	Insulin-like growth factor I
MAP2	Microtubule-associated protein
NQZ	Neurogenically quiescent zone
P	Postnatal
PBS	Phosphate-buffered saline
PFA	Paraformaldehyde
PSA-NCAM	Polysialic acid-neural cell adhesion molecule
RECA-1	Rat endothelial cell antigen-1
SGZ	Subgranular zone

Sry-related	
HMG box 2	Sox2
SRS	Systematic random sampling
ssf	Section sampling fraction
SVZ	Subventricular zone
$\text{Var}_{\text{noise}}$	Within-section variance
Var_{SRS}	Between-section variance
VEGF	Vascular endothelial growth factor

CHAPTER ONE

Overview

The generation of neurons is a fundamental process of brain development. Though once thought to be limited to the initial formation of the brain, we now know that neurogenesis is also a feature of adult mammalian brains. Adult neurogenesis is, however, not a ubiquitous phenomenon: Only the subventricular zone (SVZ) and the subgranular zone (SGZ) of the dentate gyrus (DG) of the hippocampus (HPC) are firmly established as sites supporting the generation of new neurons in adults. The process of neurogenesis in the DG is of particular interest, given this structure's important functional role most often assessed in behavioural tasks involving learning and memory (Aimone, Wiles & Gage, 2006; Shors, et al., 2002; Snyder, Hong, McDonald, & Wojtowicz, 2005).

The focus of this thesis is the discovery and characterisation of a novel, regionally-specified niche within the adult rat DG that consistently lacks neurogenesis (Melvin, Spanswick, Lehmann, & Sutherland, 2007b). This sub-region, referred to as the neurogenically quiescent zone (NQZ) occupies approximately 1.5% of the total volume of the DG. The experiments described in this thesis address 3 broad issues: The characterisation of the NQZ, tests of a model of early stem cell senescence in the NQZ, and the regulation of the NQZ. It is our contention that this area may provide a uniquely promising avenue to identify the molecular factors that mediate basal neurogenesis within the adult DG.

Chapter 1 of this thesis will give an overview of adult neurogenesis that is relevant to the work described herein. Chapter 2 will present a qualitative and

quantitative characterisation of the NQZ. Chapter 3 will present data that support an early age-related decline in neurogenesis as an explanation for the existence of the NQZ. Chapter 4 qualitatively describes experiments directed at determining whether neurogenesis can be induced in the NQZ by two common behavioural paradigms known to increase DG neurogenesis in general. Lastly, Chapter 5 will conclude by describing the utility of using the NQZ as a model system for delineating the cellular and molecular mechanisms mediating basal neurogenesis.

Identifying Neurogenesis-Related Cellular Phenotypes

The temporal cellular progression found in adult neurogenic regions is similar to that seen in other stem cell-containing systems (Weissman, 2000). Stem cells (typically defined as being multi-potent and self-renewing) give rise to lineage-restricted neural progenitors called neuroblasts, which ultimately differentiate into mature neurons, capable of functionally integrating into the existing circuitry (van Praag et al., 2002).

It had been a long-standing and essentially unchallenged belief that neurons and glial cells originate from distinct types of progenitors (Alvarez-Buylla, Garcia-Verdugo, & Tramontin, 2001). Though the existence of a neural stem cell in the adult forebrain had been appreciated in *in vitro* preparations (Morshead et al., 1994; Reynolds & Weiss, 1992; Richards, Kilpatrick, & Bartlett, 1992), the *in vivo* identity of this cell was not defined until several years later (Doetsch, Caille, Lim, Garcia-Verdugo, & Alvarez-Buylla, 1999; Seri, Garcia-Verdugo, Collado-Morente, McEwen, & Alvarez-Buylla, 2001). Though initially surprising, the nature of the neural stem cell has been firmly established to be a cell with several properties of astrocyte-like glial cells (Ihrle & Alvarez-Buylla, 2008). Garcia, Doan, Imura, and Sofroniew (2004) used the expression

of the viral enzyme thymidine kinase driven by the glial fibrillary acidic protein (GFAP) promoter to demonstrate the importance of this type of glial cell to the process of adult neurogenesis. This allows the selective expression of thymidine kinase in GFAP-expressing astrocytes. Thymidine kinase then converts the drug ganciclovir to a toxic metabolite that subsequently kills the GFAP-expressing cell. Using this approach, it was shown that the selective ablation of GFAP-expressing astrocytes results in the disappearance of neuroblasts and newly-generated mature neurons ultimately derived from them. Interestingly, this had the same effect in both the SVZ and the DG, suggesting that a GFAP+ cell is the stem cell in both systems.

Due to the lack of definitive markers, the current gold standard for identifying neural stem cells is a cell culture model based on their functional properties. In the neurosphere assay (Reynolds & Weiss, 1992), it can be demonstrated that cells isolated from the SVZ exhibit the two cardinal properties of all stem cells: Multi-potentiality (one cell can generate progeny of many different phenotypes) and self-renewal (the isolated cell can produce another daughter stem cell that can continue to produce differentiated progeny). Putative stem cells under these conditions form a floating ball of cells called the neurosphere. After growing the stem cell in the presence of mitogenic fibroblast growth factor 2 (FGF-2) and/or epidermal growth factor, the cell will begin to differentiate and produce many different cell types found in brain upon the removal of these factors (Steindler, 2007).

The issue of whether there is a true stem cell in the DG, as opposed to distinct glial and neuronal progenitors, has been a controversial issue. An early study by Gage et al. (1995) reported the isolation and expansion of FGF-2-responsive progenitors from the

adult rat DG that exhibited the properties of multi-potentiality and self-renewal. A subsequent study by this same group reported a similar result (Palmer, Takahashi, & Gage, 1997). Seaberg and van der Kooy (2002) subsequently made the claim that these earlier studies may have contained a critical methodological error: Because their tissue source was complete HPC, it was possible that their preparations suffered from contamination by the adjacent SVZ. When Seaberg and van der Kooy very carefully micro-dissected only HPC tissue, they were only able to find non-self-renewing, unipotent cells, suggesting that only lineage-restricted neural and glial progenitor cells are located in the HPC.

Using an adherent monolayer culture technique (as opposed to the neurosphere assay used by Seaberg and van der Kooy), Babu, Cheung, Ketternmann, Palmer, and Kempermann (2007) found that multi-potent, self-renewing cells could be isolated from the adult DG. Importantly, this study used the fluorescence generated by nestin-green fluorescent protein (GFP) mice to selectively isolate the DG without SVZ contamination.

One important issue to consider is that all cell culture-based assays are, by their nature, highly artificial. Not only are harsh dissection and enzymatic dissociations generally necessary, cell culture drastically alters the local environment experienced by the target cells. The strongest evidence supporting the contention that *bona fide* stem cells exist in the adult DG *in vivo* has been provided recently. The Sry-related HMG box 2 (Sox2) transcription factor has been suggested to be a critical element in allowing stem cells to maintain their “stemness”; in other words, to ensure self-renewal in order to maintain the pool of stem cells (Fong, Hohenstein, & Donovan, 2008; Wegner & Stolt, 2005). Sox2 over-expression maintains stem cells in their undifferentiated state and

blocking its expression in stem cells leads to differentiation. Using a combination of a Sox2-GFP transgenic mouse and viral-based lineage tracing, Suh et al. (2008) showed that individual Sox2-expressing cells in the DG can generate both neurons and glia, as well as another Sox2-expressing cell. Thus, in the *in vivo* environment, resident cells within the DG can exhibit the properties of multi-potentiality and self-renewal, indicating that the DG does in fact contain a population of true stem cells.

A major limitation in the field of neural stem cell biology is the lack of definitive immunohistochemical markers to identify them in tissue sections. However, there are some combinations of antigens that adult neural stem cells generally produce that have allowed their identification in tissue sections with some certainty. In addition to GFAP, another intermediate filament protein, nestin, has been shown to be present in cells with the characteristics of neural stem cells, including neurosphere formation (Mignone, Kukekov, Chiang, Steindler, & Enikolopov, 2004). Using the nestin-GFP mouse, Kempermann and colleagues have shown that two different subpopulations of nestin-expressing cells can be discerned within the DG: One with its cell body in the SGZ, extending a radial process through the overlying GCL (so-called type I cells), and the other with short processes extending parallel to the GCL (type II cells; Filippov et al., 2003). A short pulse with the thymidine analogue bromodeoxyuridine (BrdU), used to identify cells in the S phase of the cell cycle, revealed that type I cells rarely divide, whereas type II cells are highly proliferative (Kronenberg et al., 2003). In addition, this study reported significant electrophysiological differences between the two subpopulations. Type I cells exhibited passive membrane properties (consistent with that seen in mature astrocytes), whereas type II cells exhibited delayed-rectifying potassium

currents (consistent with an early neuronal-like phenotype; Filippov et al., 2003; Fukuda et al., 2003). Lastly, type I cells co-express GFAP, whereas type II cells do not (Kempermann, Jessberger, Steiner, & Kronenberg, 2004). As discussed above, Sox2 expression is also associated with stem cells, where it plays a critical functional role in stem cell maintenance. Importantly, Sox2 expression has been found to co-localise with GFAP⁺ and nestin⁺ cells in the DG (Ferri et al., 2004; Lagace et al., 2007) in tissue sections. Thus, it is possible to identify stem cells *in situ* using a combinatorial approach.

It is important to emphasise that none of these antigens are exclusively expressed by neural stem cells. GFAP is expressed by many mature astrocytes that do not have stem cell properties (Fukuda et al., 2003), nestin is expressed in some blood vessels (Fukuda et al., 2003), and Sox2 is expressed by some mature astrocytes (Komitova & Eriksson, 2004). Therefore, additional criteria are important to identify stem cells in tissue sections. Notably, stem cells within the DG have a morphological correlate as well.

GFAP⁺/nestin⁺/Sox2⁺, radial-like glial cells within the SGZ of the DG have radially-oriented processes that extend through the GCL and a characteristic triangularly-shaped cell body in the GCL (Filippov et al., 2003; Fukuda et al., 2003; Lagace et al., 2007). Therefore, the best approach currently available to identify stem cells at the level of tissue sections is likely a combinatorial approach.

The descendants of neural stem cells, the neuroblasts and subsequently mature neurons, can also be identified by several antigenic markers. Defined by their limited potential (i.e., they only generate neurons), and highly proliferative nature, dentate neuroblasts are characterised by their expression of the microtubule-associated protein doublecortin (DCX; Brown et al., 2003) and the polysialated neural cell adhesion

molecule (PSA-NCAM; Seri et al., 2004). DCX⁺ cells within the SGZ tend to have two distinct morphologies related to their age: Shortly after their appearance, DCX cells tend to have minimal processes that are oriented parallel to the overlying GCL, and more mature DCX-expressing cells have processes extending vertically through the GCL, (Brown et al., 2003). Subsequently, DCX⁺ cells produce mature, post-mitotic, NeuN-expressing granule neurons that migrate a short distance from the site of their generation in the SGZ into the overlying granule cell layer (GCL; Figure 1). The basic features of the different cell types relevant to neurogenesis in the DG are summarized in Table 1.

Neurogenesis in its Cellular Context: The Neurogenic Niche

An interesting area of investigation in stem cell biology is the concept of the stem cell niche. This niche, defined as the local environment in which stem cells and progenitors exist, is a critical collection of elements that regulate the behaviour of stem cells and, by extension, their progeny (Lim, Huang, & Alvarez-Buylla, 2007). The concept of the stem cell niche is by no means exclusive to neural stem cells. Discrete niches have been described in the *Drosophila* reproductive system (Xie & Spradling, 2000), the hematopoietic system (Hirao, Arai, & Suda, 2004) and the intestinal system (Yen & Wright, 2006), to name a few. Within adult neurogenic regions, the niche includes a variety of elements such as vasculature, cell-cell and cell-matrix interactions, and the presence of specific growth factors.

A testament to the powerful regulatory effects of the local environment in the brain can be demonstrated by the fact that glial progenitor cells isolated from the normally non-neurogenic spinal cord can be transplanted into neurogenic regions such as

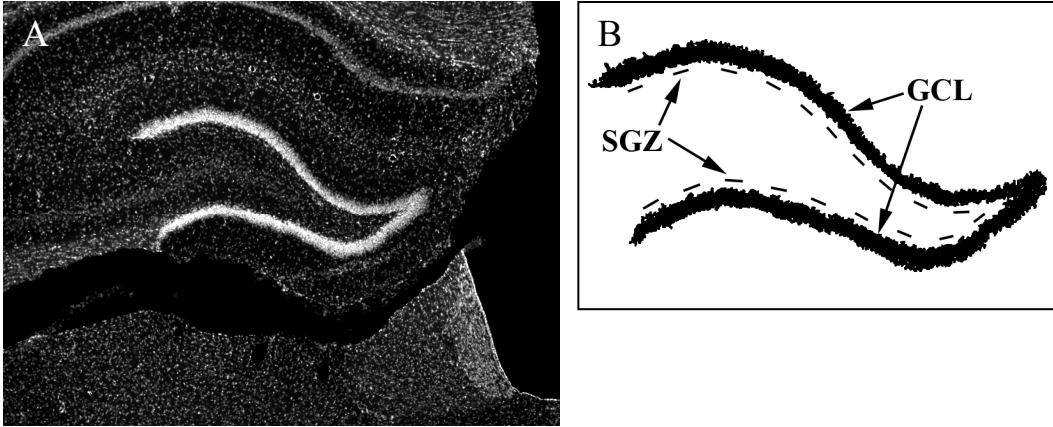


Figure 1. The DG is a site of adult neurogenesis. An image of the DG is shown in (A), and a schematic representation (B), showing the position of the mature granule cells in the granule cell layer (GCL), and the germinal zone, the subgranular zone (SGZ), immediately beneath. Neural stem and progenitor cells are generated in the SGZ. These cells subsequently produce mature granule cells which subsequently reside in the overlying GCL.

Table 1

Key characteristics of the major cell types involved in neurogenesis.

Cell type	Antigens expressed	Proliferative?	Location
Stem cell	Nestin, GFAP, Sox2	Yes (infrequent)	SGZ
Neuroblast	DCX, PSA-NCAM	Yes (frequent)	SGZ/GCL
Neurons	NeuN	No	GCL

the SVZ, where they can ultimately give rise to both neurons and glia (Shihabuddin, Horner, Ray, & Gage, 2000).

A critical component of the neural stem cell environment is the local vasculature. In a detailed anatomical analysis, Palmer, Willhoite, and Gage (2000) demonstrated that most of the dividing cells in the adult DG are found in close proximity to blood vessels. In fact, more than 1/3 of the cells that are proliferating are endothelial cells. Thus, the process of neurogenesis occurs against a spatially-related background of angiogenesis, and this association may be critical for the regulation of neural stem cell behaviour and regulation.

Direct evidence exists for a functional interaction between vasculature and neurogenesis. Shen et al. (2004) demonstrated, in cell culture, that embryonic and adult neural stem cells undergo symmetric divisions (i.e., they self-renew) only when co-cultured with endothelial cells. These data suggest that endothelial cells might secrete factors necessary to maintain the stem cell phenotype. The identity of these factors *in vivo* has not yet been elucidated.

Local interactions between different cell types and between cells and the extracellular matrix have also been shown to regulate neurogenesis within the niche. Most of our knowledge of these niche components has come from studies in the SVZ. GFAP+ astrocytes and PSA-NCAM+ cells in the SVZ express components of the Notch signalling system (Givogri et al., 2006), whose role in mediating cell fate via direct cell contact are well known in many developmental contexts (Carlson & Conboy, 2007).

Liu, Wang, Haydar, and Bordey (2005) demonstrated a negative feedback loop with the SVZ system, whereby neural progenitors begin to synthesise and secrete the

neurotransmitter gamma amino butyric acid (GABA) as a result of spontaneous depolarisations. GFAP+ stem cells subsequently exhibited inward GABA-induced chloride currents. Interestingly, this resulted in the decreased proliferation of the stem cells, suggesting an intrinsic mechanism that could regulate the number of neurons ultimately generated in the SVZ.

GABA has also been shown to exert control over neurogenesis in the DG. Tozuka, Fukuda, Namba, Seki, and Hisatsune (2005) demonstrated that nestin-expressing stem cells respond to GABA released from HPC interneurons. Due to the inverse gradient of chloride in DG stem cells, GABA resulted in their depolarization and a subsequent increase in the number of new neurons generated. This study is particularly interesting, given that it provides a link between the network activity in the HPC and the process of neurogenesis.

A Myriad of Factors Modulate Neurogenesis

Major emphasis has been placed on elucidating the molecular elements that regulate neurogenesis. A typical experimental approach to identifying these elements is to expose an animal to a particular factor and determine whether neurogenesis has been modulated. As a result, a very long and often disparate list of regulators have been collected, some of which act to positively influence neurogenesis, and others act as negative regulators. These modulators encompass similarly large categories, including growth factors, drugs, pathological states, ageing, and specific behavioural experiences.

It is not possible or pertinent to the current work to provide a comprehensive overview of these modulators. Therefore, only those factors that are relevant to the current thesis will be discussed.

Growth Factors and Neurogenesis

Several growth factors have been shown to regulate neurogenesis and are likely to be critical components of the niche. An interesting property of many of these agents is that they tend to act on discrete stages of the neurogenic process.

It has been suggested that FGF-2 is a critical factor in maintaining the stem cell state. After the initial expansion of stem cells in the neurosphere assay in the presence of FGF-2, stem cells then rapidly differentiate in response to its withdrawal (Steindler, 2007). In further support of this contention, Chen, Tung, Li, Iqbal, and Grundke-Iqbal (2007) have shown that FGF-2-treated HPC progenitor cell cultures exhibited an increase in nestin expression and a concomitant suppression of neurogenesis, indicative of its role in maintaining stemness. Convincing *in vivo* data from Zheng, Nowakowski, and Vaccarino (2004) in FGF-2 null mice, suggested that FGF-2 may be responsible for maintaining the pool of slowly dividing neural stem cells in the SVZ.

Multiple studies have suggested that FGF-2 may have differential effects in the SVZ and SGZ, and these influences may be dependent on age. Specifically, they reported that, although peripheral or intraventricular injections of FGF-2 resulted in increased mitosis in the DG during development, it had no detectable effect on mitosis in the adult DG (Cheng, Black, & DiCicco-Bloom, 2002; Kuhn, Winkler, Kempermann, Thal, & Gage, 1997; Wagner, Black, & DiCicco-Bloom, 1999). This is in contrast to its effects in the adult SVZ, where it tripled the number of mitotic cells.

However, a recent study has demonstrated that intraventricular injections of much higher concentrations of FGF-2 did result in increases in DG proliferation, as well as a significant increase in the number of DCX+ neuroblasts and enhanced dendritic growth

(Rai, Hattiangady, & Shetty, 2007). Interestingly, this study was conducted with rats that were 12 months of age and, combined with the fact that Wagner et al. (1999) and Cheng et al. (2002) had previously suggested developmental-specific effects of infused FGF-2 on DG neurogenesis, it is likely that cells in the adult DG remain responsive to FGF-2, but simply require much higher levels to be effective.

Other growth factors can also modulate neurogenesis. Specifically, VEGF increased neurogenesis *in vitro* and *in vivo* after intraventricular infusion (Jin et al., 2002). Given that VEGF is best known for its ability to stimulate angiogenesis (Cébe-Suarez, Zehnder-Fjallman, & Ballmer-Hofer, 2006) and that neurogenesis in the DG is linked to angiogenesis, VEGF is likely to be a critical, multi-functional element within the neurogenic niche.

The administration of exogenous insulin-like growth factor I (IGF-I) has also been shown to be a positive regulator of neurogenesis (Aberg, Aberg, Hedbacker, Oscarsson, & Eriksson, 2000). When infused peripherally, IGF-I resulted in a doubling of the number of BrdU+ cells in the DG after 1 day, as well as increase in the number of surviving/differentiating neurons, as assessed by the increased number BrdU+ cells expressing calbindin, another marker of mature neurons in the DG. In addition, intraventricular infusions of IGF-I have also been shown to increase the number of BrdU+ cells in the DG and to increase the number of mature neurons subsequently generated (Lichtenwalner et al., 2001). This same study, however, revealed a selective effect on proliferation in the aged DG: Despite eliciting increased numbers of proliferating cells, there was no net increase in the proportion of BrdU+ cells co-expressing NeuN.

Behavioural Experience can Modulate Neurogenesis

Two of the best characterised behavioural procedures that stimulate DG neurogenesis are the housing of animals in enriched environments, and allowing animals to freely exercise on a running wheel. Interestingly, though each of these experiences can result in net increases in DG neurogenesis, they appear to do so by selectively acting on discrete phases of the process (Olson, Eadie, Ernst, & Christie, 2006).

The term “enriched environment” can have a variety of specific definitions, but generally consists of a relatively large living area in which many different animals are able to interact with each other, and with a variety of “toys”, such as plastic tubes, nesting materials, and ropes. Regardless of the specific design in a given study, the goal is to provide a rich social and physical environment relative to animals raised in standard “shoe box” cages. Several studies have reported increased levels of neurogenesis in mice in response to environmental enrichment. Kempermann and colleagues have shown that, although proliferation levels determined in animals killed 1 day after BrdU injection revealed no difference between mice in enriched environments versus animals in control cages, enrichment animals killed one month after BrdU injections had larger numbers of BrdU+ cells in the DG (Kempermann, Kunh, & Gage, 1997). This suggests that environmental enrichment may have a selective effect on mediating longer-term survival of adult-generated cells, but little effect at the level of proliferation. This conclusion was further supported by the fact that, one month after BrdU administration, enriched animals had more mature granule cells than controls. Subsequent work has reported similar results in rats (Nilsson, Perfilieva, Johansson, Orwar, & Eriksson, 1999).

Physical exercise, in the form of running in a wheel, also induces DG neurogenesis in rodents. However, as opposed to the preferential effect of environmental enrichment on cell survival, voluntary wheel running appeared to have a relatively selective effect on proliferation, with a slight increase in the survival of newly-generated neurons (van Praag, Kempermann, & Gage, 1999). Interestingly, the effects on proliferation may be transient, peaking at about 3 days after the initiation of running, and returning to control levels by 1 month (Kronenberg et al., 2006). The number of DCX+ neuroblasts, on the other hand, continued to increase over time.

Interestingly, exercise is associated with increased levels of several growth factors. FGF-2 levels have been shown to be increased both centrally (Gomez-Pinilla, Dao, & So, 1997) and peripherally (Campuzano et al., 2002) in response to exercise. In addition, both VEGF (Schobersberger et al., 2000) and IGF-I (Trejo, Carro, & Torres-Aleman, 2001) serum levels have been shown to increase as a result of exercise.

Two studies have provided key information with regards to the molecular mechanisms that mediate the neurogenic effects of wheel running. Trejo et al. (2001) showed that peripheral administration of a function-blocking IGF-I antibody to running rats completely prevented the exercise-induced increase in neurogenesis. Similarly, Fabel et al. (2003) has subsequently demonstrated that the blockade of peripheral VEGF also prevented running-induced increases in DG neurogenesis. As noted by Olson et al. (2006), no such study has been conducted to determine FGF-2's effects.

These studies highlight the fact that growth factors produced outside the brain during exercise can exert significant influences on central neurogenesis, providing a critical link between an animal's behavioural experience and adult neurogenesis.

Neurogenesis and Ageing

In addition to the many positive regulators of neurogenesis, there are also factors that act to reduce neurogenesis. Particularly interesting are those that decrease neurogenesis in the absence of exogenous treatments. The strongest known endogenous negative regulator of neurogenesis is age (Kempermann, 2006). Certainly, this temporal component could also be considered as another aspect of the neurogenic niche (Nern & Momba, 2006).

Neurogenesis in the DG decreases strongly with age. Though several groups have reported decreased cell proliferation, differentiation, and survival by middle age in rodents (e.g., Kuhn, Dickinson-Anson, & Gage, 1996; Nacher, Alonso-Llosa, Rosell, & McEwen, 2003), only one group has quantified these alterations with the correct usage of rigorous stereological methods. They reported decreases in both acute proliferation and in the absolute number of DCX+ neuroblasts in the DG (Rao, Hattiangady, & Shetty, 2006). This down-regulation does not appear linearly across age: The number of DCX+ cells in the DG remained constant until about 7.5 months of age, after which it decreased by almost half by 9 months of age. By 12 months of age, the number of DCX+ neuroblasts was reduced to 25% of that seen at 7.5 months.

In the context of the neurogenic niche, several factors could, in principle, account for age-related declines in neurogenesis. One obvious explanation is that there may be a disappearance of DG stem cells capable of supporting this process. However, in a subsequent publication by Shetty, they convincingly demonstrated that there is no decrease in the number of stem cells across age. Specifically, Hattiangady and Shetty (2008) showed that there was no difference in the absolute number of GFAP+ radial glial

cells in the SGZ or the number of Sox2+ radial glial cells, or the proportion of cells co-expressing these markers across age. Importantly, there was a significantly decreased proportion of Sox2+ stem cells in the DG that were actively dividing: The fraction of Sox2+ cells that co-expressed the endogenous cell cycle marker Ki-67 in young animals (4 months old) was 25%, by middle age, 8% and, in aged (24 months) animals, 4%. Remarkably, the proportion of BrdU+ cells at both 6 hours and 12 days after injection is not altered with ageing, suggesting no impairments in relatively short-term cell survival across age (Rao et al., 2006). Based on these data, Hattiangady and Shetty suggested that age-related declines in DG neurogenesis are likely explained by the dramatically increased quiescence of local stem cells.

One obvious explanation for the decreased proliferation of stem cells in the aged DG is that the local niche may be deficient in factors that stimulate proliferation. In support of this contention, several growth factors that have been shown to be pro-neurogenic in the DG (including FGF-2, VEGF, and IGF-I) exhibit decreases during ageing that parallel the decrease in neurogenesis (Shetty, Hattiangady, & Shetty, 2005). Of direct relevance to the current thesis is the demonstration by this group that, although the number of GFAP+ cells does not decrease with age, the proportion of GFAP+ cells that co-express FGF-2 declines by about 30% from young animals to middle age, and by a subsequent 50% in aged animals. Thus, GFAP+ astrocytes in the DG from ageing brains appear to be deficient in their production of FGF-2. This is an intriguing result, given the proposed role of FGF-2 in allowing stem cells to retain their stem cell phenotype (Yeoh & de Haan, 2007), and its mitogenic properties under some circumstances.

An instructive role for some of these growth factors in the context of ageing has also been demonstrated. Intraventricular infusion of FGF-2 and heparin-binding epidermal growth factor-like growth factor (HB-EGF) dramatically increased the degree of proliferation and the number of DCX+ neuroblasts in aged mice relative to non-treated, age-matched controls (Jin et al., 2003). As discussed above, the intraventricular infusion of FGF-2 (Rai et al., 2007) and IGF-I (Lichtenwalner et al., 2001) have also been reported to have neurogenesis-stimulating effects in aged animals.

The ability to “rescue”, to some extent, levels of neurogenesis in the aged DG by growth factor treatments implies that DG stem cells retain the ability to produce new neurons, but that they are simply missing the critical stimulation provided by growth factors. Not surprisingly, exposing aged mice to running wheels (Kronenberg et al., 2006) and enriched environments (Kempermann, Kuhn, & Gage, 1998) results in increased levels of neurogenesis. Thus, the underlying mechanisms that cause declines in neurogenesis with age appear to be related to alterations in the neurogenic niche over time; specifically, the loss of expression of several critical growth factors.

Identifying the Molecular Mechanisms Mediating Basal Neurogenesis in the Adult DG

Arguably, the most important goal of studies of adult neurogenesis is to define the molecular mechanisms that allow it to occur. The very long list of diverse modulators of neurogenesis that has been collected (e.g., Abrous, Koehl, & Le Moal, 2005) highlights a central weakness in studies of neurogenesis: The necessarily single or limited multi-factor approaches have led to a broad collection of data from which a coherent picture has not emerged, though recent attempts to create such a picture have been made (e.g., Hagg, 2005).

The studies described above primarily involve the assessment of the effects of exogenous treatments on the process of neurogenesis. This approach clearly has yielded important insights into relevant mechanisms, but an ideal approach would involve methods that are capable of discovering the molecular mechanisms that regulate basal neurogenesis under non-experimentally-induced conditions. Rather than the “serial search” methods employed thus far, methods of transcriptional profiling (e.g., microarrays) and comparative proteomics have the potential to provide a parallel search for relevant critical factors *en masse*: Comparing gene and protein expression profiles between two essentially identical areas that differ only in the processes of interest (i.e., proliferation and differentiation) would provide ideal starting material for such an approach.

The current work defines an anatomically discrete and consistent area within the young adult rat DG that meets such criteria. This thesis qualitatively and quantitatively describes and characterises this area, which is referred to as the NQZ. This zone is constant across rats with respect to its size and position, and is identified by its constitutive lack of signs of neurogenesis, including proliferation and differentiation. Additionally, the NQZ has many elements that are critical to the neurogenic niche, including stem cells and vasculature, and appears qualitatively similar to other areas of the DG that do exhibit constitutive neurogenesis. Furthermore, this area exhibits a developmental profile that is consistent with age-related declines in neurogenesis, and can be induced to undergo neurogenesis under some conditions, but not others.

Given that this area appears to be phenotypically similar to other areas of the DG, yet critically different with respect to the processes involved in neurogenesis, it is

the contention of this work that the NQZ may offer the best model system currently available for identifying the molecular mechanisms responsible for mediating basal neurogenesis.

CHAPTER TWO

The HPC and DG Neurogenic Heterogeneity

The DG is one of the principal subfields of the HPC. The major synaptic connections of the DG form essential parts of the classic “tri-synaptic loop” within the HPC. The HPC receives its major excitatory input from the entorhinal cortex. The incoming fibres (referred to collectively as the perforant path) release the excitatory transmitter glutamate onto the dendrites of granule cells. The axons of granule cells then synapse on pyramidal cells in area CA3 via the mossy fibre pathway. CA3 neurons subsequently send projections, the Schaffer collaterals, to area CA1. Most of the output of HPC is from CA1 back to the entorhinal cortex, as well as to subiculum, thalamus, and hypothalamus (Amaral & Lavenex, 2007). The CA3-CA1 cell layers form a distinct C-shaped structure that interlocks with the boomerang-shaped DG (Figure 2). Within the rodent brain, the HPC takes on a characteristic “twisted banana” shape, with its long axis running anteroposteriorly within the brain.

Several studies have revealed that the DG, both anatomically and functionally, is not a homogenous structure. For example, the anterior and posterior DG differ with respect to the discrete origins of inputs from the entorhinal cortex. This has functional implications due to the fact that the entorhinal cortex is a site of unimodal and polymodal sensory information from other cortical structures (Mohedano-Moriano et al., 2008). Anterior DG receives visuo-spatial sensory information (Burwell & Amaral, 1998), whereas olfactory sensory information appears to be more evenly distributed across the longitudinal axis (Sahay & Hen, 2007).

In this light, it is puzzling that, with regard to the process of neurogenesis, the DG

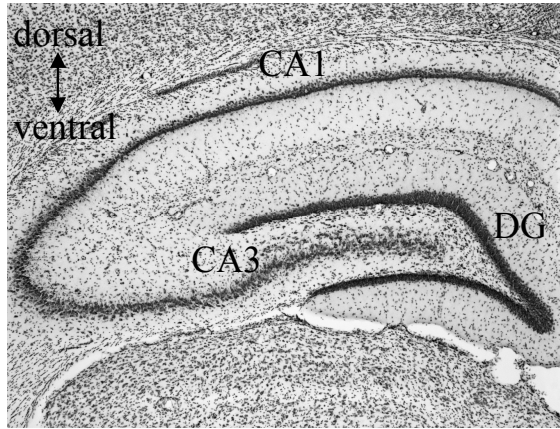


Figure 2. The general organization of the HPC as seen in the coronal plane. Inputs to the granule cells of the dentate gyrus (DG) project from the entorhinal cortex. Granule cells then project to CA3, and CA3 projects to CA1.

is generally examined as a whole, under the assumption that this process occurs homogeneously along its anteroposterior axis. Some studies have examined regional differences with regard to the number of cycling cells across the DG. For example, Kempermann, Gast, Kronenberg, Yamaguchi, & Gage (2003) have reported that the dorsal blade of the DG in mice tends to have more cycling cells than the ventral blade. Two additional studies have demonstrated antero-posterior differences in the DG with respect to neurogenesis in terms of its response to anti-depressant treatments (Banar, Soumier, Hery, Mocaer, & Daszuta, 2006) and stress (Jayatissa, Bisgaard, Tingstrom, Papp, & Wiborg, 2006).

Of particular relevance in the current context is an explicit statement made recently with regard to the distribution of DCX+ neuroblasts along the anteroposterior DG axis: “the distribution of new granule cells is consistent across the anteroposterior extent of the DG, as the number of new granule cells in the anterior and posterior segments of the DG are similar” (Rao & Shetty, 2004, p. 244).

This chapter reports the identification and subsequent quantitative and qualitative descriptions of a unique area of the adult rat DG that consistently lacks any signs of neurogenesis. This area, referred to as the NQZ, was the result of a serendipitous discovery made during the course of preparing routine histological material for the analysis of neurogenesis, and is anatomically identified by its consistent and contiguous lack of DCX+ cell bodies in the dorsal blade of the anterior DG.

We contend that, by virtue of the fact that the NQZ is very similar to other areas of the DG that do undergo constitutive neurogenesis, it offers a unique opportunity to

exploit the methods of differential gene expression to identify the molecular mechanisms of stem cell proliferation and differentiation.

Much of the data in this chapter was published previously in Melvin et al. (2007b). However, it also includes a substantial amount of data not yet published.

Materials and Methods

Animals

Adult (defined here as 3 – 3.5 months of age) male Long-Evans hooded rats were obtained directly from Charles River Laboratories (Wilmington, MA) or from local breeding stocks in the Department of Neuroscience. In all studies in this chapter, animals were housed in pairs. All procedures were conducted in compliance with the standards of the Canadian Council on Animal Care and the University of Lethbridge Animal Welfare Committee.

Perfusions

Animals were euthanized with a lethal injection of Euthansol (Schering-Plough, ~ 0.7 mL of a 150 mg/mL stock), and then transcardially perfused with ~ 150 ml of 0.1 M phosphate-buffered saline (PBS), pH 7.4, followed by 200 mL of 4% paraformaldehyde (PFA) in 0.1 M PBS. Brains were removed and post-fixed in 4% PFA in PBS for 24 hours at 4 °C. This solution was then replaced by 30% sucrose in PBS containing 0.02% sodium azide as a preservative.

Histology

All brains were cut at a thickness of 40 µm on a freezing sliding microtome (American Optical, model #860; Buffalo, NY). For quantitative studies, brains were cut with a section sampling fraction (ssf) of 1/5 or 1/7 (i.e., 5 or 7 series of sections); for

qualitative studies, brains were bisected and each hemisphere was collected independently with a ssf of 1/12. From this, series from each individual brain (with the hemisphere chosen randomly) were then pooled to allow a ssf of either 1/6 or 1/4, while maintaining equal spacing between series. For example, pooling series # 1 and # 7 allowed a ssf of 1/6 to be sampled from the original ssf of 1/12; similarly, series # 1, # 5, and # 9 were pooled from one brain to achieve a ssf of 1/4. Importantly, the first series number was chosen at random, thus determining the subsequent series and maintaining their equal spacing. This form of sampling is known as systematic random sampling (SRS). During the cutting process, sections were collected into PBS containing 0.02% sodium azide. Sections were then stored at 4°C until used.

Antibodies

Information about the sources, host species, label, and dilutions used in this series of studies are provided in Table 2.

BrdU Administration

To determine the number of acutely proliferating cells in the DG, animals were injected with a single intraperitoneal injection of 150 mg/kg of BrdU (Sigma, product # B5002) mixed at a concentration of 50 mg/ml in 0.9% sterile saline with heating. Animals were then injected after sufficient cooling. Control animals (one per cage, randomly selected) were injected with an equivalent volume of 0.9% saline. All animals were perfused 3 hours after BrdU administration.

Immunohistochemistry

Immunohistochemistry was conducted as free-floating sections, using 0.1 M PBS with 0.3% Triton X-100 as a diluent in all cases. Incubation times were 24 hours or 48

Table 2

Antibodies, dilutions, and suppliers used in immunohistochemical experiments.

Antibody	Host species	Dilution	Supplier, catalogue #
<i>Primaries (all IgG subclass)</i>			
NeuN	Mouse	1:1,000	Chemicon, MAB 377
S100 β	Rabbit	1:15,000	Swant, 37
BrdU	Rat	1:100	Oxford Biotechnology, OBT0030
DCX	Goat	1:500	Santa Cruz Biotechnology, sc-8066
Ki-67	Rabbit	1:1,000	Novocastra, NCL-Ki-67p
GFAP	Guinea pig	1:6,000	Advanced Immuno, 31223-200
GFAP	Mouse	1:20,000	Sigma, G3893
Nestin	Mouse	1:75	BD Pharmingen, 556309
MAP2(a+b)	Mouse	1:2,000	Sigma, M1406
RECA-1	Mouse	1:500	Serotec, MCA970R
Sox2	Goat	1:1,000	Santa Cruz Biotechnology, sc-17320
<i>Secondaries (all IgG subclass)</i>			
Anti-rabbit/ Alexa 488	Donkey	1:250/ 1:1,000	Molecular Probes, A21206
Anti-mouse/ Alexa 488	Donkey	1:500/ 1:1,000	Molecular Probes, A21202
Anti-rat/ Alexa 488	Chicken	1:600	Molecular Probes, A21470

Table 2

(continued)

Antibody	Host species	Dilution	Supplier, catalogue #
Anti-rabbit/ Cy3	Donkey	1:500/ 1:1,000	Jackson, 711-165-152
Anti-goat/ Biotin	Donkey	1:6,000	Jackson, 705-065-147
Anti-guinea pig/ Biotin	Donkey	1:2,000	Jackson, 706-065-148
Anti-goat/ Cy5	Donkey	1:1,000	Jackson, 705-175-147
<i>Tertiaries</i>			
Streptavidin/ Alexa 568	N/A	1:500	Molecular Probes, S11226

hours for primary and secondary antibodies, and 1 hour for tertiary reagents where necessary. All incubations were carried out at room temperature with rotation. Every immunohistochemical procedure included labeling for DCX (except Sox2, which was raised in the same species as the DCX antibody) to serve as a definitive reference for the boundaries of the NQZ. All immunohistochemical preparations were stained with the nuclear stain 4',6-Diamidino-2-phenylindole dihydrochloride (DAPI; Sigma, D9542) at a final concentration of 300 ng/mL. Control experiments included the incubation of sections in the absence of primary antibodies and incubation of additional sections with secondary or tertiary reagents alone. For multiple labelling experiments, control experiments involved treating sections independently with each primary antibody, and subsequent treatment with the inappropriate secondary antibodies. Particular combinations were only used when the complete absence of cross reactions were confirmed.

BrdU immunohistochemistry required several antigen retrieval steps before being subjected to the immunohistochemical protocol as described above. First, the tissue was incubated in a solution of 2x saline sodium citrate buffer in 50% formamide at 65 °C for 2 hours. After two rinses in 2X saline sodium citrate buffer, sections were subsequently placed into 2N HCl at 37 °C for 30 minutes. After several rinses in PBS over approximately 1.5 hours, the tissue was then subjected to antibodies as appropriate.

Sections were mounted out of PBS and coverslipped with a glycerol-based antifade reagent (9.8% polyvinyl alcohol, 2.5% 1,4-diazabicyclo[2.2.2]octane, 24% glycerol in 0.1M Tris-HCl, pH 8.3; all obtained from Sigma).

Quantification of BrdU and Ki-67+ Cells

The number of BrdU+ cells was analyzed by taking one series from each animal, and double labeling for DCX and BrdU. The number of BrdU+ cells was counted in each section under 40x magnification (NA 0.75), excluding the uppermost focal plane to minimize the number of double counts that occur as a result of split nuclei at the cut surface (Kronenberg et al., 2006). Note that this is not strictly unbiased, but represents a practical compromise given the technical limitations under which these experiments were conducted. The number of cells counted was then multiplied by the inverse of the respective ssf to obtain an estimate of the total number of BrdU+ cells per brain. The number of Ki-67+ cells was calculated similarly. Since the injection of BrdU has no effect on the number of Ki-67+ cells (Student's *t* test, with < 0.05 deemed as statistically significant), BrdU injected and saline injected animals were pooled for Ki-67 data.

In order to compare the relative frequencies of BrdU and Ki-67+ cells in the NQZ with non-NQZ regions of DG, these numbers were normalized to the total volume of the GCL (minus the volume of the NQZ; see section below on volume estimation) in each brain. The average number of expected cells of each type was then scaled to the volume of the NQZ to discern the number of immunoreactive cells that were expected to be present in this region.

Epi-fluorescence Microscopy, Confocal Microscopy, and Image Analysis

Signals were subsequently analyzed under appropriate filters using a Zeiss Axioskop2 MotPlus microscope and images were captured at 1360 x 1036 pixels using a QImaging Retiga EXi CCD camera (Burnaby, British Columbia). No digital image enhancements were used in the data presented here.

For the determination of co-localization, sections were imaged at a size of 512 x 512 pixels using a 60x water immersion lens on a Nikon C1 confocal microscope. Co-localization was confirmed by collecting z stacks at a z interval of 1 μm using sequential scans without averaging frames. Stacks were then examined by rendering to allow a 180° view. Great care was taken to optimize immunohistochemical signals for each combination of antibodies such that no digital image enhancements beyond linear gain changes were made. For image presentation, confocal stacks were colour separated using the RGB split function in ImageJ 1.38x (<http://rsb.info.nih.gov/ij/>), and are presented as flattened 8 bit grayscale images.

Cavalieri Volume Estimates

The volumes of the DG as a whole and the NQZ specifically were estimated using the Cavalieri estimator (Schmitz and Hof, 2005). The estimates in this experiment were conducted semi-manually, as these were conducted before the acquisition of an automated stereology system. Briefly, all images were captured on the Zeiss Axioskop2 MotPlus microscope at 2.5x using DAPI to delineate the GCL and DCX to delineate the NQZ. For the 1/7 ssf, an average of 18 sections were obtained through the entire DG, and for the 1/5 an average of 27 sections were obtained. Importantly, the series selected from each animal was selected randomly by using the random number generator plug-in in Microsoft Excel. This is a critical pre-requisite for the Cavalieri estimator to provide an unbiased estimate of volume. Images of each section were obtained and imported into ImageJ. Using the grid plug-in, a grid was generated consisting of a series of equidistant crosses with an area per point of 0.02 mm^2 . The grid was then randomly “thrown” across each image to ensure a random interaction between the crosses and the GCL, another

necessary pre-requisite for the Cavalieri estimator to return an unbiased estimate. The number of points hitting the GCL on DAPI-stained images of all sections through the DG was counted. A similar approach was used for quantifying the volume of the NQZ.

An unbiased estimate of volume (V_{est}) for each animal was calculated according to the Cavalieri estimator:

$$V_{\text{est}} = \sum P \cdot a(p) \cdot T. \quad (1)$$

where $\sum P$ is the sum of points counted across all sections, $a(p)$ is the area per point of the grid (0.02 mm^2 in this case) and T is the distance between sections, which is itself the product of the section thickness (0.04 mm) and the inverse of the relevant ssf. The total volume of the GCL, as well as the volume of the GCL found associated with the NQZ, were subsequently calculated.

In order to determine what proportion of the DG was occupied by the NQZ, a volume fraction was calculated by the following expression:

$$\frac{V_{\text{NQZ}}}{V_{\text{GCL}}}. \quad (2)$$

where V_{NQZ} is the estimated volume of the NQZ, and V_{GCL} is the estimated volume of the GCL as calculated above.

The precision of the GCL estimates was estimated by calculating the coefficient of error (CE) for each brain using the method of Gundersen (Gundersen et al., 1999; Bermejo et al., 2003). With a ssf of 1/5 or 1/7 employed here, the CE of the volume

estimates of the NQZ were not possible, as the Gundersen CE estimator requires at least 3 sections for its calculation. The relevant equations and their derivation are explained in detail in the Results section of this chapter. As these data were collected before the acquisition of our automated stereology system, all CEs were calculated manually.

Three Dimensional (3D) Modelling

In an effort to model the anatomical position and shape of the NQZ within the anterior DG, we co-labelled every second section from one animal with DCX to define the NQZ and DAPI to define the general pattern of the GCL. Images of each channel from each section were captured on a Zeiss Axioskop2 MotPlus as described above and imported into 3D Studio Max (<http://usa.autodesk.com/adsk/servlet/index?siteID=123112&id=5659302>) and were digitized by tracing the signals from the DAPI (blue) and DCX (red) channels on each section separately. Digitized signals from each section were then compiled and rendered to produce a 3D “hinged” movie of the NQZ in which the ventral blade swung out to reveal the dorsal blade. Images presented in this chapter represent screen captures from the movie.

Results

The Size and Location of the NQZ

We found a subregion of the DG that consistently lacks signs of neurogenesis. The NQZ is characterised by the contiguous lack of DCX⁺ cell bodies in the dorsal blade of the DG at its anterior pole. Along the anteroposterior axis of the DG, the NQZ extends approximately 700-800 μm . With reference to the rat brain atlas of Paxinos and Watson (1998), this corresponds to positions of approximately 2.28 mm posterior to Bregma to

3.00 mm posterior to Bregma. Figure 3 illustrates the spatial pattern of DCX immunoreactivity in sections of anterior DG (Figure 3 A'-C'), with DAPI-stained images of the corresponding sections in Figure 3 A-C from one animal, with each section spaced 240 μm apart. As more posterior sections are analyzed, the NQZ progressively 'fills in' with DCX+ cells in a lateral-to-medial gradient (note the arrows in Figure 3), after which DCX+ cell bodies are present relatively homogeneously across both blades of the DG.

The NQZ in 3 Dimensions

In order to gain a 3D conceptualization of the NQZ, we reconstructed, from every second section in one animal, the anterior pole of the DG. By outlining the general pattern of the GCL in the dorsal and ventral blades of the DG using DAPI as a reference (blue in Figure 4), we imported images into 3D Studio Max and traced the GCL in several coronal sections. To discern the NQZ, using the lack of DCX+ cell bodies as an operation definition, we also traced the pattern of DCX immunoreactivity (red in Figure 4). When the images were compiled, a "hinged" model of the anterior DG was constructed, using the point of convergence of both blades (the apex) as the hinge. Figure 4 A shows a front-on view of both blades of the DG. Figure 4 B shows the DG with the ventral blade swung open, revealing the size and position of the NQZ within the dorsal blade.

The NQZ forms a quasi-triangularly shaped wedge in the anterior DG, with the pattern of DCX+ cell bodies converging on the apex in more posterior sections in a lateral to medial fashion. In sections further posterior to those shown in Figure 3, DCX+ cell bodies are present essentially "shoulder-to-shoulder" across both blades of the DG.

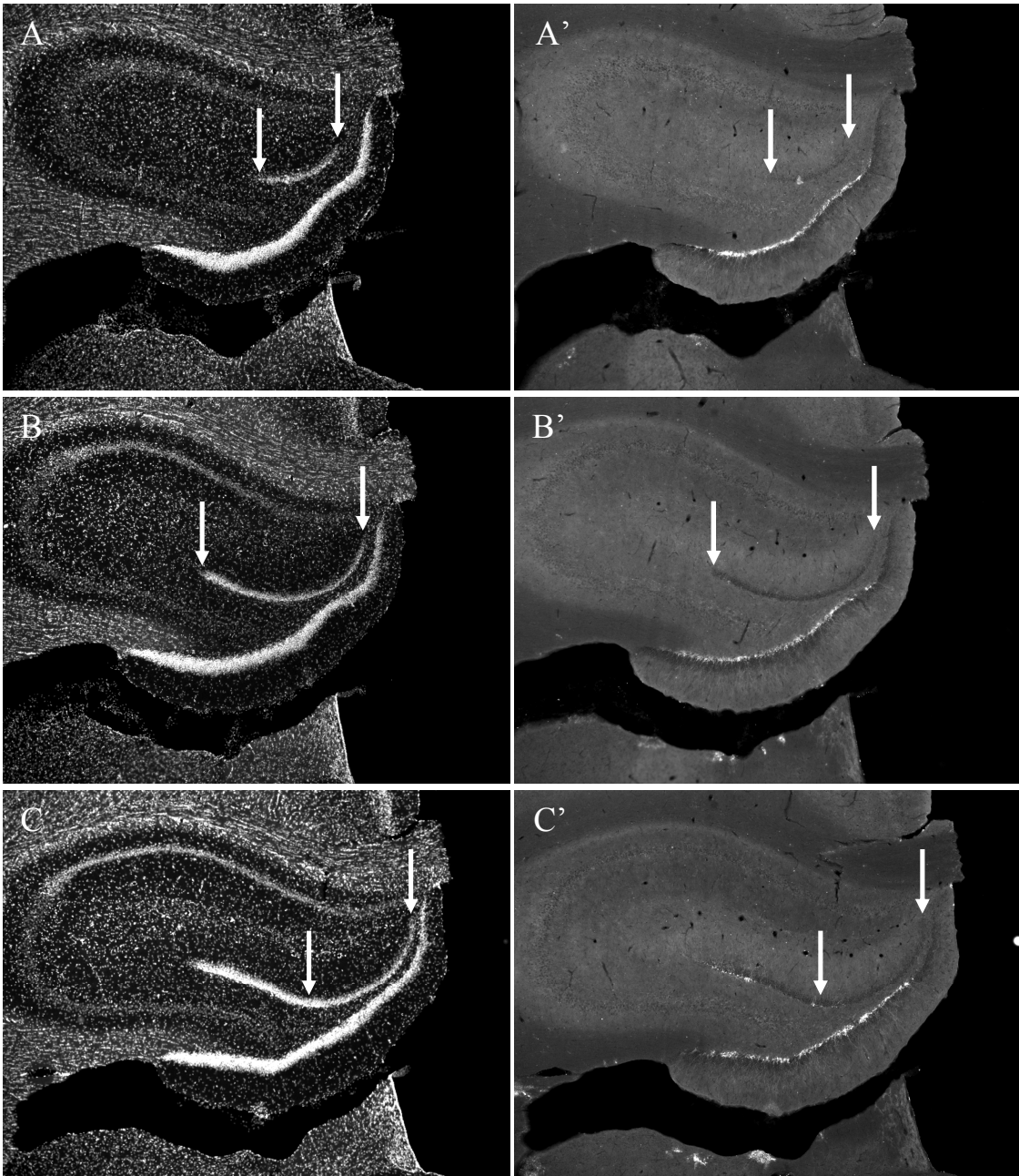


Figure 3. The anatomical location of the NQZ. The NQZ is located in the dorsal blade of the DG, and is defined by its consistent lack of DCX+ expression, between the arrows in (A', B', and C'). Corresponding DAPI-stained sections are shown in panels (A, B, and C). The inter-section interval is 240 μm .

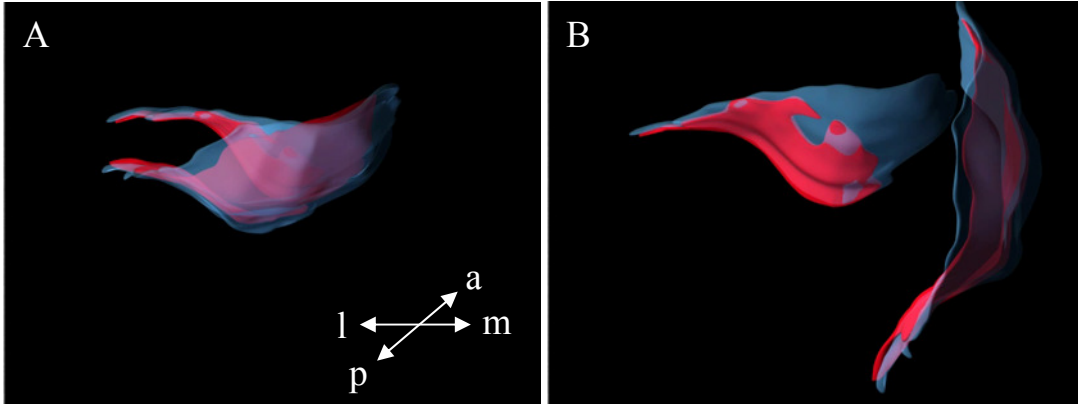


Figure 4. A 3D reconstruction of the NQZ. Using every second section, images from one animal were rendered from anterior DG tissue sections and assembled with 3D Studio Max software. In this “hinged” model of the anterior DG from one animal, the dorsal and ventral blades are seen in blue and the pattern of DCX immunoreactivity is seen in red. Both blades are viewed from the front in (A). In (B), the ventral blade is swung out, exposing the position of the NQZ in the dorsal blade (blue without red). Its shape is quasi-triangular, and fills in from lateral to medial as more posterior sections are analyzed. The lower case letters in (A) denote the orientation of the images (a is anterior, p is posterior, m is medial, and l is lateral).

The Anatomical Size and Location of the NQZ is Consistent Between Animals

Using the Cavalieri estimator in combination with point counting to estimate the areas on individual sections, the GCL exhibits a typical bimodal distribution of areas when examined in the coronal plane. The distribution of GCL areas by section, from anterior (section 1) to posterior, from 3 animals is depicted in Figure 5. Using a ssf of 1/7, the NQZ is present in only two sections near the anterior pole of the DG. Despite small variations in areas, the position and size of the NQZ within the DG is remarkably similar between animals.

Stereological Design and Sampling Error Prediction

In order to characterise the size and position of the NQZ within the DG with high precision, we used rigorous stereological methods; specifically, the Cavalieri volume estimator (Mouton, 2002). There are two primary advantages to this approach in the current context. To begin with, it provides an unbiased estimate of the volume of a structure of any shape from a series of essentially 2D tissue sections. Secondly, methods exist which allow predictions of the precision of any one such estimate to be made. Thus, the Cavalieri method is perfectly suited to map the size and location of the NQZ within the DG with a pre-defined level of accuracy.

It is important to note that this estimator is strictly unbiased only if specific histological prerequisites are met. Unbiased in this context means that, with increasing sampling intensity, a given estimate converges on the true value of the given parameter (Mouton, 2002). In practice, this entails that the entire structure under consideration (referred to as the reference space) must be available for sampling and all parts must have the same probability of being included in the sample. Because the particular series of

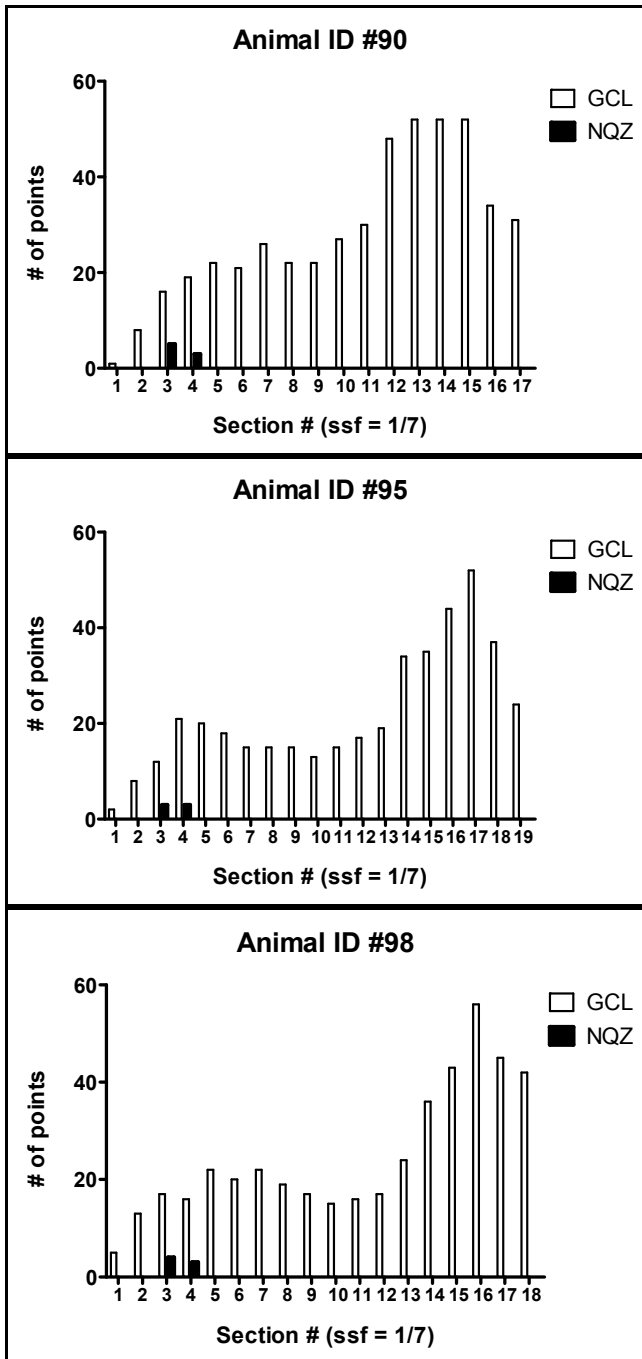


Figure 5. The neurogenetically quiescent zone (NQZ) is similar in size and position across animals. An area (proportional to the # of points, section 1 is most anterior) plot from three individual animals. When every seventh section is samples, the NQZ is located in only two sections near the anterior pole relative to entire granule cell layer (GCL).

tissue sections from each animal was selected at random, and the grid of crosses used to estimate area was thrown across each section at random, this method provided a mathematically unbiased estimate of volumes for the DG and the NQZ.

The specific histological prerequisites necessary for the Cavalieri method to be of use are as follows. To begin with, tissue sections must be collected using SRS, which in practice means that the sections must be collected with a random start position outside the structure of interest, with all subsequent sections located at equidistant intervals. Second, the entire reference space (the DG and the NQZ) must be available for sampling, with no sections missing or damaged. Third, the identification of the structures of interest must be unambiguously identifiable. In order to meet these last two requirements, a significant amount of work went into optimizing the tissue preparation, sampling intensities, and immunohistochemical procedures to facilitate unbiased and efficient estimates.

A critical strength of a stereological approach to mapping the size of the NQZ is the availability of formulae for predicting the precision of individual volume estimates. Predicting the precision of stereological estimates is generally valuable only when the ultimate goal is the application of inferential statistics (Cruz-Orive et al., 2004): Knowing which sources of variance are dominant contributors to the overall variance allows one to modify the sampling parameters such that the study provides sufficient statistical power to detect a particular effect size. This was not the goal of the volume estimates presented in this chapter, but there is nevertheless substantial merit to making use of precision estimates in the initial characterisation of the NQZ: Sampling with sufficient intensity (decided *a priori* to be within +/- 5% of the true value) will allow us to infer with some confidence both the size and position of the NQZ, and to determine how constant these

features are across animals. This information will undoubtedly be valuable when trying to access the NQZ *in vivo*. As the methods used to estimate the precision of Cavalieri estimates are not familiar to most neuroscientists, their origins, meaning, and derivations will be briefly described as they pertain to the data presented in this chapter.

The precision of the volume estimates was estimated by calculating the CE using the Gundersen method, which is based on Matheron's quadratic approximation (Gundersen & Jensen, 1987; Gundersen et al., 1999). The CE is an individual statistic calculated on volume estimates obtained from an individual animal. This is converted to a group statistic by calculating the group mean CE, which is calculated squaring the CEs from each animal, taking the average, and subsequently taking the square root of this value.

In contrast to the simple random sampling commonly employed in many histological studies (i.e., "representative sections"), the sampling method used in stereology (SRS) represents a form of dependent sampling: Once a tissue series or a point on a grid is chosen at random, the position of all subsequent sections or grid points fall at equidistant intervals. The use of SRS is inherently much more efficient than simple random sampling. In fact, the variance of a sample mean under simple random sampling decreases by $1/n$ for n independently collected samples. In contrast, the variance of a sample mean collected using SRS decreases by $1/n^2$ (Melvin, Poda, & Sutherland, 2007a; West et al., 1991). Thus, the benefit afforded by using strict SRS is that much less sampling is required to achieve a given level of precision. However, predicting the precision of SRS estimates is significantly more complex than that required for predicting the precision of simple random sampling estimates.

Calculating the CE is important in designing appropriate sampling intensities in stereological studies for two reasons. Not only does it allow an estimate of how far a given volume estimate is likely to be from its true value (as if it were determined by infinite sampling), but it also allows one to assess the relative contribution of sampling error by variance splitting. This provides important information with regards to how many sections to sample (i.e., what the ideal ssf is) and what size of grid to use in order to obtain estimates of a given precision efficiently.

When the volume of an object is estimated with the Cavalieri estimator, sampling occurs at two levels. Because a subfraction of the total available sections is randomly chosen for volume estimation (a ssf of $1/7$, for example), there is a ‘between-sections’ SRS sampling error associated with the process (denoted as Var_{SRS}). Similarly, because a subsample of the total area across each section is conducted using a grid of equidistant points with a known spacing, there is also a ‘within-section’ component to the error (known as the ‘noise’ component, Var_{noise}). Each of these sources of error is an independent contributor to the total CE, and knowing these quantities allows one to assess which level contributes most to the overall error. This is helpful in determining whether the sampling additional sets of sections or decreasing the spacing of the grid within the existing sections will be most helpful in reducing measurement error (Nyengaard, 1999).

The total CE is the sum of both of these sources of error, and is given by the following expression:

$$CE_{\text{total}} = \frac{\sqrt{\text{Var}_{\text{SRS}} + \text{Var}_{\text{noise}}}}{\sum P}. \quad (3)$$

The contribution of the between-sections variance is given by:

$$\text{Var}_{\text{SRS}} = \frac{3(A - \text{Var}_{\text{noise}}) - 4B + C}{\alpha}. \quad (4)$$

where A is the sum of points counted in a given section multiplied by itself, B is the sum of points counted in one section multiplied by the next section, and C is the sum of points in a given section multiplied by the section two away. Thus, this component of the CE calculation attempts to model how the areas vary across an individual animal when, for example, every seventh section is sampled. The smoothness constant α of the object under study as it is “seen” by the sampling intensity employed (Slomianka & West, 2005). In Gundersen’s CE approach, α can take on values of either 12 or 240, corresponding to a smoothness constant of 0 or 1, respectively. If the areas of essentially any biological object are estimated using every possible section (i.e., a ssf of 1), and the sections are relatively thin, then the distribution of areas by section will be inherently smooth. With regards to the CE, this would tend to approach an m value of 1, making the denominator 240 in Equation 4. As one takes samples of sections that are farther apart, the smoothness of the areal distribution decreases, and the smoothness constant is better approximated by using a value of 0. This results in a change in the denominator of equation 4 to 12. The choice of the appropriate smoothness factor for a given sampling intensity is not always straightforward. However, for the ssfs of 1/5 or 1/7 used in the data reported in this chapter, an α value of 240 was used (Slomianka & West, 2005).

The second component contributing to the total CE is the variability due to the fact that the area of the individual sections was estimated using a random throw of a grid of equally-spaced points. It is an attempt to estimate how much the measurement of the areas on the sections would likely vary if the grid was thrown randomly an infinite number of times: A grid with more sparsely-placed points will generate greater variability between multiple throws.

This component, $\text{Var}_{\text{noise}}$, is dependent on the shape of the object under consideration (Gundersen & Jensen, 1987; Howard & Reed, 2005). In order to gauge the complexity of an object's shape, a dimensionless shape factor is calculated by the following expression:

$$\frac{b}{\sqrt{a}} \quad (5)$$

where b is the average boundary length of the object, and a is the average area of the object (which is estimated inherently in the Cavalieri estimator). In the current experiments, the boundary length was estimated by randomly rotating each digital image of the GCL within one animal using ImageJ. A series of parallel lines a known distance apart (T) was then randomly thrown across each image, and the total number of intersections (I) between these lines and the GCL was counted. b was then estimated by:

$$b = \frac{\pi}{2} \cdot T \cdot I \quad (6)$$

Substituting the value obtained for b into Equation 5 resulted in a shape factor value of 18 for the DG. This was used in all subsequent CE calculations for the DG.

The shape factor is then incorporated as a term into the following expression to estimate how much variability arises from using grid throws to estimate the areas across all sections:

$$\text{Var}_{\text{noise}} = 0.0724 \cdot \frac{b}{\sqrt{a}} \cdot \sqrt{n \cdot \sum P}. \quad (7)$$

where 0.0724 is a constant for point lattices in quadratic arrangements (Tang et al., 2003), n is the total number of sections from a particular animal, and $\sum P$ is the total number of points counted across all sections. An example of a CE calculation from one animal is shown in Table 3.

The mean CE for this group of 10 animals was originally reported as 4.7% (Melvin et al., 2007b). However, in subsequent discussions with Dr. Lutz Slomianka, a noted authority in this area, it was determined that, at the relatively intense ssfs used in this study, a recalculation would likely provide a better approximation of the true precision. The revised mean CE calculated for the same data set as published in Melvin et al. is 2.5%, suggesting that the precision of these estimates was higher than originally reported. Importantly, this altered CE value does not affect the values obtained for volumes. These recalculate values are shown in Table 4.

It is important to note that not all stereologists agree that the Gundersen method used in the vast majority of stereological studies, including this one, is the best available to calculate CEs (Schmitz & Hof, 2000). This is reflected in the output of many

Table 3

A sample volume estimate and CE calculation from animal #98.

Section #	# points total GCL	A	B	C
1	5	25	65	85
2	13	169	221	208
3	17	289	272	374
4	16	256	352	320
5	22	484	440	484
6	20	400	440	380
7	22	484	418	374
8	19	361	323	285
9	17	289	255	272
10	15	225	240	255
11	16	256	272	384
12	17	289	408	612
13	24	576	864	1032
14	36	1296	1548	2016
15	43	1849	2408	1935
16	56	3136	2520	2352
17	45	2025	1890	-
18	42	1764	-	-
Sums	445	14173	12936	11368

Table 3

(continued)

$$\begin{aligned}V_{\text{est}} &= 445 * 0.02 \text{ mm}^2 * (0.04 \text{ mm} * 7) \\ &= 2.492 \text{ mm}^3\end{aligned}$$

$$\begin{aligned}\text{Var}_{\text{noise}} &= 0.0724 * 18 * (18 * 445)^{0.5} \\ &= 116.635\end{aligned}$$

$$\begin{aligned}\text{Var}_{\text{SRS}} &= (3(14173-116.635) - 4 * 12936 + 11368)/240 \\ &= 7.471\end{aligned}$$

$$\begin{aligned}\text{CE}_{\text{total}} &= (116.635 + 7.471)^{0.5}/445 \\ &= 0.025\end{aligned}$$

Table 4

Quantitative estimates of the volume of the granule cell layer (GCL), the neurogenically quiescent zone (NQZ), the NQZ volume fraction, and estimates of precision.

Animal #	GCL volume (mm ³)	CE	NQZ volume (mm ³)	Volume fraction
90	2.705	0.023	0.045	0.016
91	2.932	0.019	0.024	0.008
92	2.363	0.027	0.039	0.017
93	2.386	0.026	0.034	0.014
94	2.335	0.030	0.056	0.024
95	2.330	0.026	0.034	0.014
96	2.447	0.025	0.017	0.007
97	2.094	0.028	0.050	0.024
98	2.492	0.025	0.039	0.016
99	2.768	0.020	0.024	0.009
Mean	2.485	0.025	0.036	0.015
CV	0.100	-	0.342	0.401

professional stereology software packages, which offer at least four CE calculation results with any one volume or cell count estimate. However, a recent study by Slomianka and West (2005) compared a number of CE estimators with empirically determined CEs in the rat HPC. Their findings support the contention that the Gundersen method performs remarkably well over a wide range of commonly-employed sampling intensities.

By calculating the two variance components as in Equations 4 and 7, it is apparent that, at this sampling intensity, the within-section variance (i.e., the noise) was the dominant source contributing to the measurement error. Thus, if greater precision were required, much greater gains could be accomplished by increasing the within section sampling (decreasing the grid spacing) rather than sampling additional sections. However, because the overall CE was already very low, no additional sampling was needed.

It is important to emphasize that the CE has no biological meaning, but is simply an estimate of precision. However, it is useful in determining additional group statistics, such as the biological variability (BV) in the parameter of interest (Mouton, 2002). The total variation within a given set of data is the standard deviation (SD) normalized to the mean, and is given by the coefficient of variation (CV):

$$CV = \frac{SD}{\text{mean}}. \quad (8)$$

The CV is itself the sum of BV and the measurement error (CE):

$$CV^2 = BV^2 + \text{mean } CE^2. \quad (9)$$

Given that the mean CE for the group can be predicted as above, and the CV is calculated from Equation 8, we can then obtain an estimate of the BV. The various ratios of each of the above terms can then provide useful information with regard to whether measurement error or inherent biological variation between animals is the dominant source of variability. For the GCL, measurement error accounted for only 6% of the total variability ($\text{mean } CE^2 / CV^2$), with BV accounting for the additional 94%. Thus, if a more precise estimate were required, obtaining additional animals would be more effective than additional sampling within the existing group of animals.

Importantly, the precision of the NQZ volume estimates could not be calculated under the sampling intensity used here. This is because the Gundersen estimator requires a minimum of 3 sections. However, because the NQZ was typically only present in two sections at the sampling intensity employed in this study, its associated CE and BV could not be calculated. Nevertheless, it is likely that the great majority of error associated with the NQZ measurements was due to relatively light sampling. Given that a relatively large number of animals were used to estimate these parameters, and the fact that the Cavalieri method is unbiased, the mean volume of the NQZ obtained is very likely a reasonable estimate. The volume estimates of the GCL and the NQZ, the GCL CE, and the NQZ volume fraction are presented in Table 4.

The mean volume of the NQZ was 0.036 mm^3 , which represents a volume fraction of 0.015. Thus, the NQZ represents 1.5% of the total DG volume. Note that the CV for the GCL volume was very low (less than 10%), indicating a relatively low degree of total variability across all animals. The CV for the NQZ volume (34%) and the volume fraction (40%) were higher in relative terms, which is a consequence of the fact that, at a ssf of 1/5 or 1/7, only 2 sections contain the NQZ. In addition, the grid spacing used for the NQZ was the same as that used for the total GCL volume. In this situation, a low number of points will land in the NQZ.

The NQZ is Consistently Devoid of Cell Proliferation

The absence of DCX+ neuroblasts in the NQZ leaves open the possibility that cells of other lineages may be produced locally. In an effort to address this hypothesis, we used two additional markers of lineage-independent cell proliferation: BrdU and Ki-67.

To determine proliferation levels using BrdU, animals received a single injection of 150 mg/kg of body weight, a dosage previously shown by Mandyam, Harburg, and Eisch (2007) to label the entire population of cells in the DG cycling at the time of administration. Animals were then sacrificed 3 hours after the injection, and cells were counted across the DG. Surprisingly, we did not observe any BrdU+ cells in the NQZ in any animal, suggesting that it lacks locally proliferating cells.

The argument could be made that, given the small volume of the NQZ and the relative infrequency of BrdU+ cells in the DG in general, the lack of BrdU+ cells in the NQZ is the result of the insufficient sampling of a rare event. To address this issue, we expressed the data in terms of the number of BrdU+ cells that would be expected to be

present in the NQZ, given its volume and given the average density of BrdU+ cells in all other areas of the DG. Using this quantitative approach, the expected number of BrdU+ cells expected to be present in the NQZ if it had a similar density of cycling cells as non-NQZ areas was 29. Again, we never observed a single cell in the NQZ of any animal (Figure 6).

The use of BrdU alone as an index of proliferation is not without its limitations, and conclusions based solely on it should be seen as tenuous at best (Eisch & Mandyam, 2007). Given that it is only incorporated into cycling cells that are in the S phase at the time of injection, BrdU will always underestimate the number of cells proliferating at any given time. Accordingly, one could argue that our injection simply did not happen to hit any local cells in the S phase. This is an unlikely explanation, but we sought further support for the contention that the NQZ does not contain any cells in the cell cycle by using an endogenous marker of proliferation.

A similar quantitative approach was taken using the expression of the endogenous cell cycle-related protein Ki-67. Ki-67 is expressed during all phases of the cell cycle, though its subcellular distribution can change with specific phases (Endl & Gerdes, 2000). The number of Ki-67+ cells expected in the NQZ using this approach was 66. As with BrdU, we observed essentially no actively cycling cells in the NQZ (Figure 7). It should be mentioned that we found potentially two Ki-67+ cells in the region of the NQZ, both of which were in the same animal. However, it is certainly possible that these cells may in fact be more properly classified as belonging to the hilus with respect to their position, given that the definition of the SGZ at the light microscopic level is rather loose (i.e., 2-3 nuclear or cell diameters below the granule cell layer; Kempermann, 2006).

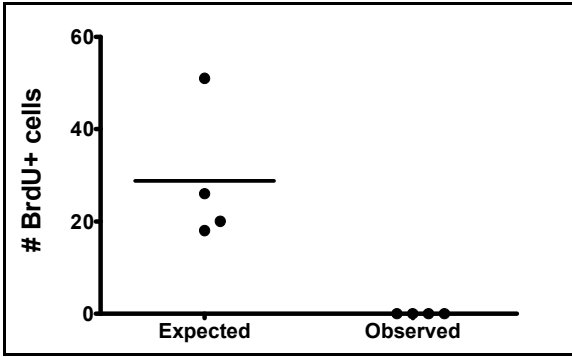


Figure 6. The NQZ lacks cellular proliferation as assessed by bromodeoxyuridine (BrdU). The bar within each group indicates the group mean, and each symbol within a group represents a single datum point.

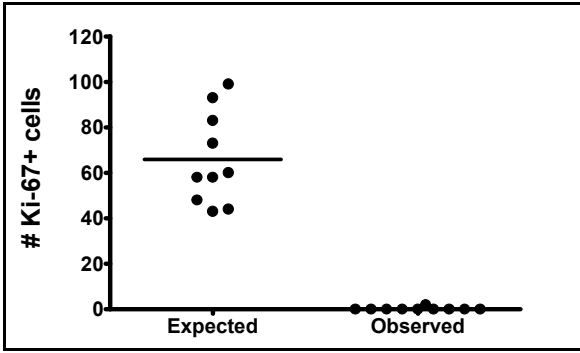


Figure 7. No Ki-67+ cycling cells were observed in the NQZ.

Taken together, these data support the contention that the NQZ lacks cell proliferation.

The NQZ Contains Similar Cell Types to Other Areas of the DG

Given its lack of cell proliferation and DCX⁺ neuroblasts, it is possible that the NQZ may simply represent a fundamentally unique portion of the DG in other domains as well. Thus, we sought to determine whether there were any qualitative differences between the NQZ and “typical” areas of the DG that do undergo constitutive neurogenesis.

Since mature granule neurons and glial cells can also be considered components of the neurogenic niche, we next characterised the general cellular constituents present within the NQZ. Though the GCL associated with the section of NQZ depicted in Figure 8 A is generally thinner than adjacent non-NQZ areas that do exhibit constitutive neurogenesis, the size and distributions of NeuN⁺ mature granule neurons appeared qualitatively similar (Figure 8 B). In addition, there was no evidence for a lack of mature astrocytes, as inferred by the presence of S100 β ⁺ cells (Figure 8 C). Confirmation of the location of these cells in the NQZ was confirmed by the absence of DCX⁺ cell bodies in the dorsal blade (Figure 8 D).

The dendrites of mature granule neurons in the DG have characteristic features. Specifically, their dendrites extend into the overlying molecular layer, where they ramify to various degrees depending on the location of their cell bodies within the GCL (Green & Juraska, 1985). In order to determine whether the general organization of dendrites arising from granule cells in the NQZ was similar to non-NQZ areas, we used the dendritic marker microtubule-associated protein 2 (MAP2). There are several isoforms of MAP2 that are developmentally regulated in terms of their expression. However, the A

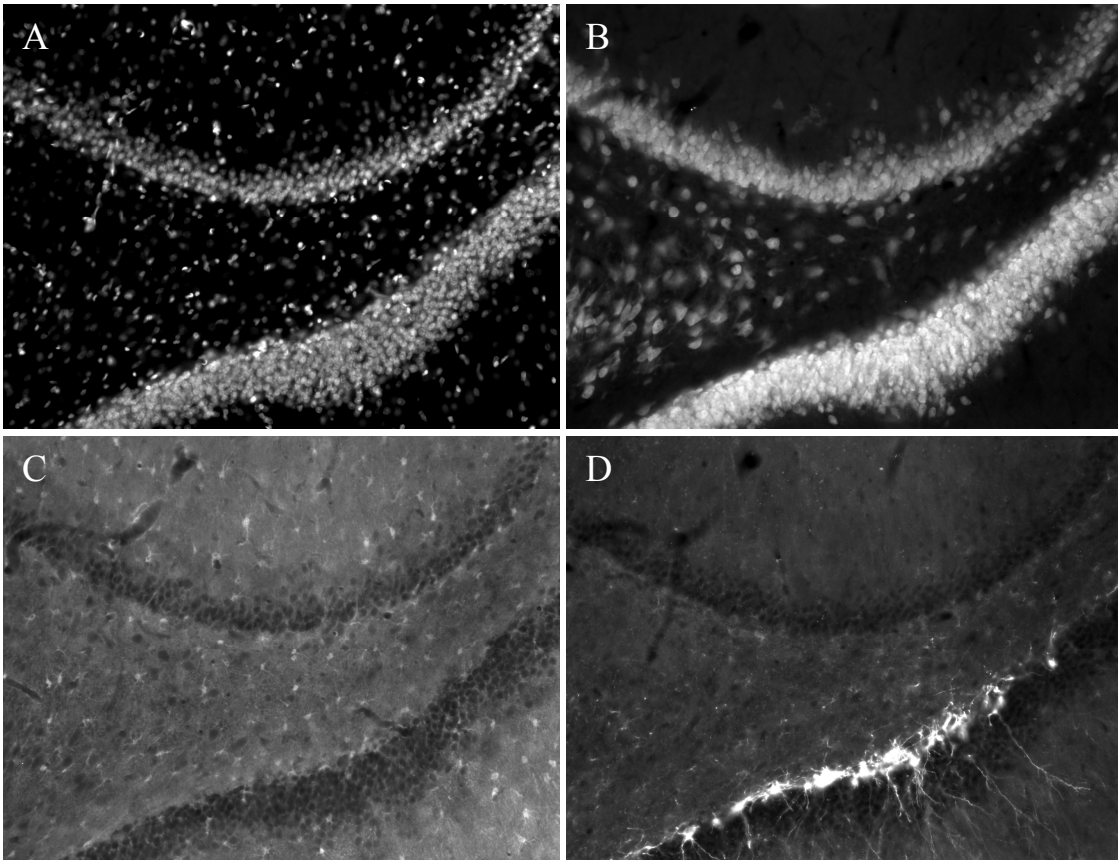


Figure 8. The distribution of mature neurons and glial cells is qualitatively similar in the NQZ versus non-NQZ areas. Though the GCL associated with the NQZ (the top blade in these images) is thinner than non-NQZ areas (bottom blade; DAPI label in A), it contains both NeuN+ neurons (B) and S100 β + astrocytes (C) that are qualitatively similar. The DCX signal for this section is shown in (D).

and B high molecular weight isoforms of MAP2 are known to be highly expressed in the dendrites of many adult neurons, including granule cells (Kwak & Matus, 1988). In contrast, the lower molecular weight C isoform is known to have a prototypical expression pattern during neural development, exhibiting a general decrease in expression, including in the DG (Jalava, Lopez-Picon, Kukko-Lukjanov, & Holopainen, 2007). The antibody we employed here recognized the A and B isoforms of MAP2, but not MAP2C. The dendritic structure of granule neurons in the NQZ is qualitatively similar to other areas of the DG (Figure 9).

The NQZ Contains Stem Cells

Given the importance of the local environment to the neurogenic niche, a logical prediction is that if an area of the DG is consistently devoid of neurogenesis, it may be because it is deficient in one or more elements critical to the process of neurogenesis, or there is a local factor that is a potent inhibitor.

As discussed in Chapter 1, stem cells themselves are central elements of the neurogenic niche. Thus, one explanation for the lack of neurogenesis in the NQZ is that perhaps the NQZ contains no resident stem cells to initiate process. In order to address this issue, we sought to detect type I stem cells using a variety of antigenic markers. Type I cells that give rise to DCX⁺ cells in the DG express GFAP, nestin, and Sox2 (Ferri et al., 2004; Lagace et al., 2007; Suh et al., 2008). In addition, they also tend to have a triangularly-shaped cell body present in the SGZ (Fukuda et al., 2003; Namba et al., 2005). Qualitative analysis of NQZ sections revealed that individual cells that co-express GFAP (Figure 10 B) and nestin (Figure 10 C) are present in the SGZ. Importantly, these cells have the typical triangularly-shaped cell body (arrows).

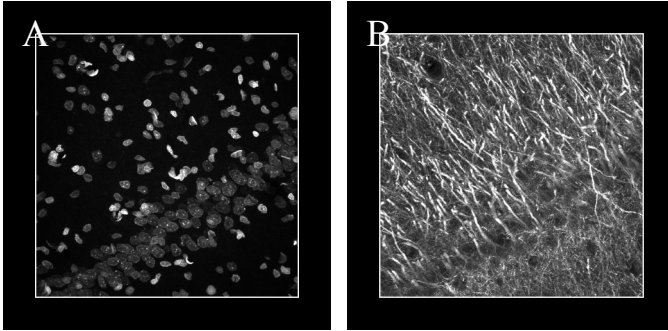


Figure 9. Granule neurons in the GCL of the NQZ have a typical dendritic morphology. Note the extension of MAP2+ dendritic trees into the overlying molecular layer (B). The general position of the GCL using DAPI in (A).

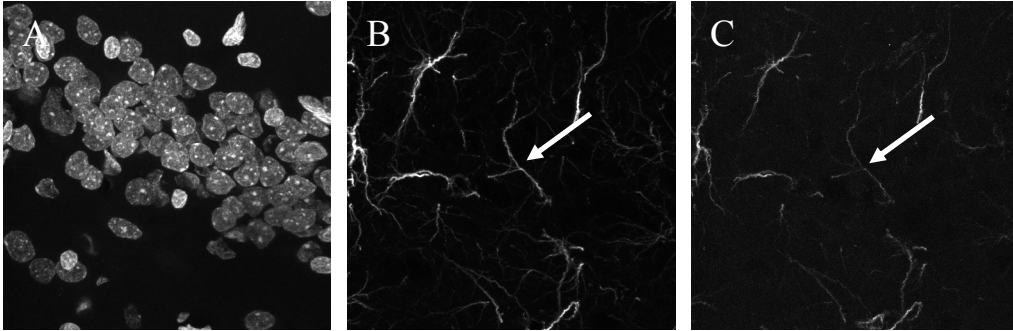


Figure 10. The SGZ of the NQZ contains stem cells. The arrows highlight an individual cell with a triangularly-shaped cell body that expressed GFAP in (B) and nestin (C). These criteria are consistent with the identification of stem cells using immunohistochemistry.

Given that the expression of Sox2 is also associated with neural stem cells, we employed Sox2 immunohistochemistry in an attempt to further support the contention that the NQZ contains resident stem cells. Figure 11 highlights a GFAP+ cell (Figure 11 B) that also expresses Sox2 (Figure 11 C) in the SGZ of the NQZ. Additionally, this cell also has the triangularly-shaped cell body that is a characteristic feature of DG stem cells (arrows). Thus, by all currently accepted immunohistochemical definitions of a neural stem cell in the DG, they are in fact present in the NQZ.

The NQZ Contains a Vascular Network

As discussed in Chapter 1, the process of neurogenesis occurs in close association with the local vasculature (Palmer et al., 2000). A subsequent study by Shen et al. (2004) provided evidence *in vitro* that endothelial cells that line the walls of vasculature may release factors that stimulate both the proliferation and differentiation of neural stem cells. Thus, a possible explanation for the lack of neurogenesis in the NQZ is that it is relatively avascular.

To address this possibility, we mapped the distribution of blood vessels in the NQZ using an antibody to the rat endothelial cell antigen 1 (RECA-1). RECA-1 detects an antigen specifically expressed in endothelial cells (Duijvestijn et al., 1992), and thus serves as a general marker of the vasculature. Figure 12 illustrates an example of several RECA-1+ vessels within the NQZ, including an individual vessel that spans the GCL, subsequently bi-furcating at the border with the SGZ (Figure 12 B). Though not quantified in this study, the density of vessels in the NQZ appeared similar to adjacent non-NQZ regions of the DG (Figure 13).

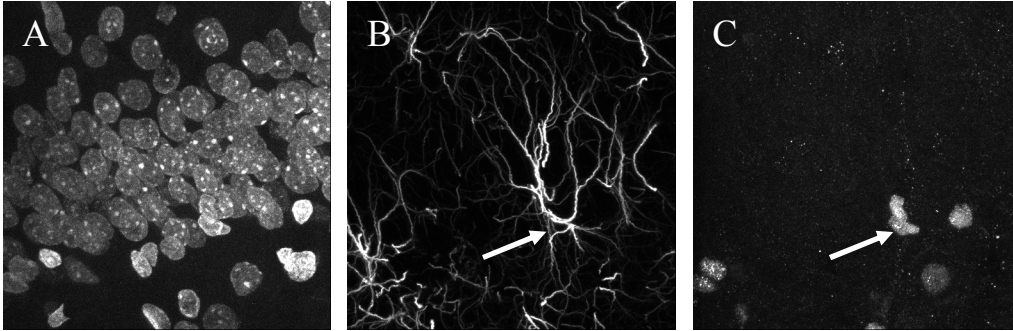


Figure 11. The SGZ contains stem cells. The NQZ contains GFAP+ stem cells (B) with a triangular cell body in the SGZ that co-expresses Sox2 (C). The general outline of the GCL of the NQZ is shown in (A) using DAPI.

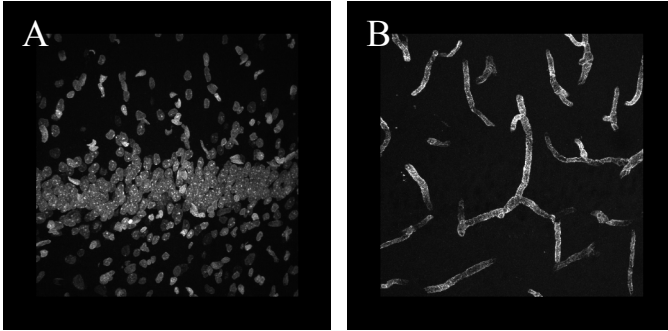


Figure 12. The NQZ contains vasculature. RECA-1+ vessels extend across the GCL and bifurcate at the SGZ (B). The corresponding DAPI-stained sections is shown in (A).

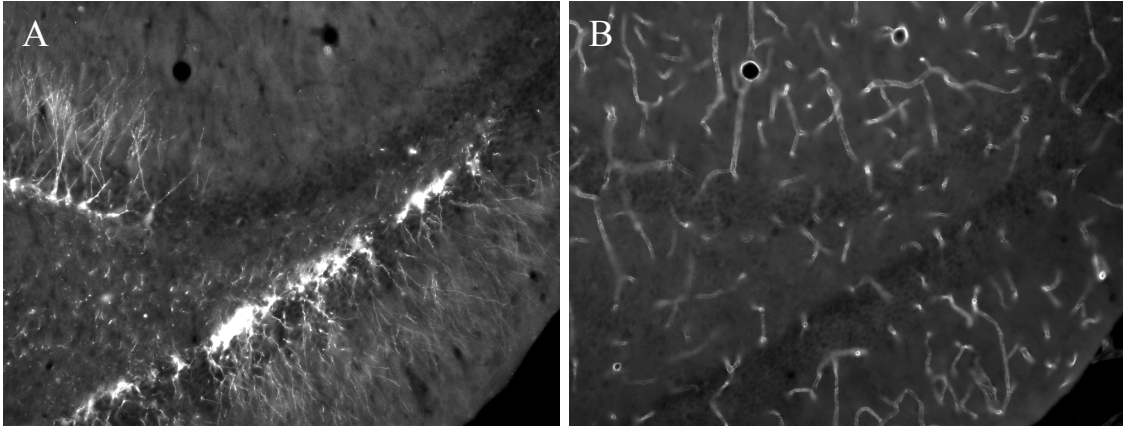


Figure 13. The density of blood vessels in the NQZ is similar to non-NQZ areas of the DG. The absence of DCX in the dorsal blade (A) identifies the NQZ, and RECA-1+ vessels are shown in (B).

Discussion

We have described and characterised the first instance of an area of the adult DG that consistently lacks neurogenesis. This quasi-triangular area is predictably present in the dorsal blade at the anterior pole of the DG, and is remarkably similar in its distribution and size between animals, occupying approximately 1.5% of the total DG volume. We do not contend that this is the only area of the dentate that does not undergo neurogenesis, but it is of particular interest because its presence in young adult animals is invariant and its location is anatomically identifiable between animals.

A number of features of the NQZ are remarkably similar to those of other non-NQZ regions of the DG that do exhibit constitutive neurogenesis. The NQZ contains a qualitatively similar distribution of key elements of the neurogenic niche, in particular granule cells and associated dendrites, glia, and blood vessels. Interestingly, it appears to differ only with respect to the process of neurogenesis: Despite the presence of local stem cells, there is a complete lack of DCX+ neuroblasts as well as all signs of local cells being engaged in the cell cycle. These results suggest that the NQZ harbours a population of stem cells that are mitotically quiescent.

Stem cell quiescence is typically defined as a state of “reversible growth/proliferation arrest” (Coller, Sang, & Roberts, 2006, p. 329). In this light, it is interesting to note that one non-experimentally-induced factor that is associated with DG stem cell quiescence is ageing, despite the persistence of similar numbers of stem cells across age (Hattiangady & Shetty, 2008).

Ageing appears to be the most potent endogenous down-regulator of neurogenesis (Kempermann, 2006). In this light, it is interesting to speculate that the NQZ described in

this paper may be related to this age-related decline in neurogenesis; specifically, this zone may represent one of the first areas to undergo stem cell quiescence. This idea generates several concrete predictions. If this hypothesis were true, DCX+ neuroblasts would be present in every region of the DG immediately after its initial formation; the NQZ would then emerge before animals reach 3 months of age, the age of the animals used in this study.

The age-related declines in neurogenesis have been suggested to be due to the lack of specific growth factors within the neurogenic niche that normally provide a permissive environment for neurogenesis (Lichtenwalner et al., 2001; Rao et al., 2006; Shetty et al., 2005). Thus, the lack of neurogenesis in the NQZ in animals of this age may be caused by an early local decline in some or all of these factors. This further predicts that neurogenesis may be inducible in the NQZ by methods that restore growth factor levels to that area. The data presented in Chapter 3 address the issue of whether the NQZ exhibits signs of “early ageing”.

CHAPTER THREE

DG Development, Ageing, and Neurogenesis

The NQZ is an area located in the dorsal blade at the anterior pole of the DG that consistently lacks neurogenesis. The question of why neurogenesis does not occur in this region in the adult presents no small problem. Indeed, this question could be addressed at multiple levels, from the behavioural to the molecular. However, the focus in the current context was to identify cellular and molecular correlates that might contribute to the explanation for the existence of the NQZ. This chapter addresses two key issues: age-related changes in the relative size of the NQZ, and whether the NQZ lacks growth factors that are known to be critical components of the neurogenic niche.

In placing the NQZ in a theoretical framework, we note several key facts about this area. To begin with, it exists “naturally”, defined here as without any acute experimental intervention. Second, the NQZ lacks signs of neurogenesis, including the expression of cell cycle-related antigens (BrdU and Ki-67) and DCX, a marker of the neuroblast phenotype. Third, the NQZ contains stem cells, but they are, by definition, mitotically quiescent. Interestingly, all of these elements are qualitatively similar to the changes that occur in the DG during ageing (Hattiangady & Shetty, 2008). Thus, it is logical to pursue an explanation of the NQZ in this context. We hypothesize that it represents a discrete region that undergoes the age-related decline in neurogenesis during adolescence before other parts of the DG.

As discussed in Chapter 1, neurogenesis in the DG decreases dramatically beginning at approximately 7.5 months of age. Rao et al. (2006) have mapped these temporal decreases using stereological methods. They reported that, although the number

of DCX+ neuroblasts in the DG from 4 – 7.5 months of age remains stable, a decline of almost 50% occurs by 9 months of age. By 10.5 months of age, the number of DCX+ neuroblasts is approximately one third of the level seen at 7.5 months and, by 12 months of age, about one quarter. A dramatic decline in the number of proliferating cells was also reported by Rao et al. The number of Ki-67+ cells at 12 months of age was about 25% of that seen in 4 month old animals, and about 12% by 24 months of age. Given that 7.5 – 12 months of age in the rat corresponds to “adult to middle-age”, this work suggests that DG neurogenesis declines before the period typically identified as senescence.

Several studies have examined the cellular and molecular changes that correlate with decreased DG neurogenesis during ageing. A number of growth factors within the neurogenic niche exhibit decreased expression that occurs in parallel with these age-related declines. For example, IGF-I, VEGF, and FGF-2 levels decrease significantly by middle age in the DG (Shetty et al., 2005), corresponding to the initial drop in the cellular signs of neurogenesis by middle age. A functional role for these growth factors in maintaining neurogenesis during ageing is supported by studies demonstrating that their infusion into the aged brain can at least partially restore DG neurogenesis to levels typical of younger animals. Treatment of animals with FGF-2 (Rai et al., 2007) and IGF-I (Lichtenwalner et al., 2001) both have strong neurogenic effects in aged animals. Thus, cells in the aged DG likely retain their sensitivity to these growth factors, and the decline in their endogenous synthesis, at least in part, explains the age-related declines in DG neurogenesis.

Given that the proportion of dividing stem cells decreases dramatically with age (though the absolute number of stem cells is similar in young and old animals), it is

interesting to speculate that the lack of critical growth factors responsible for maintaining the levels of stem cell proliferation is primarily responsible for the decline in DG neurogenesis across age (Hattiangady & Shetty, 2008). Thus, if the NQZ's existence were caused by early ageing, we hypothesised that it would exhibit decreased expression of some or all of these niche components. However, due to several technical limitations (discussed at the end of this chapter), we present data related only to the expression of FGF-2 in the NQZ.

In our original report describing the NQZ (Melvin et al., 2007b), we proposed a critical test of an “early ageing” model: The relative size of the NQZ should increase with age. However, in order to test this hypothesis, it is important to dissociate the processes of adult neurogenesis from those of the initial formation of the DG, most of which occur postnatally. Because differentiating granule neurons initially forming the GCL during development also express DCX (Tanaka, Koizumi, & Gleeson, 2006), it is possible that the lack of an NQZ at early ages could simply be due to the persistence of DCX expression from the last born granule cells that populated the GCL.

The DG, along with the cerebellum, is relatively unique in terms of brain development, since most of its principal cells (granule neurons) are generated postnatally. Several classic studies using a series of short-term tritiated thymidine survival radiograms were particularly instrumental in defining the spatial and temporal aspects of DG development. Granule neurons are generated during development from three successively-generated germinal zones. The primary germinal zone, referred to as the dentate notch, is located near the ventricular surface lateral to the future DG, and becomes mitotically active at embryonic day 16 (E16; Altman & Bayer, 1990b). Putative

stem cells from this region then migrate a small distance medially to form the secondary germinal matrix at E18, located between the dentate notch and the future DG. The secondary germinal matrix produces the first granule cells that will inhabit the DG, forming an initial “outer shell” of the GCL just before birth. This germinal zone then decreases in mitotic activity in the late embryonic and early postnatal period, ultimately giving rise to the tertiary germinal matrix located in the hilus, an area in between CA3 and the developing GCL of the DG. The tertiary matrix contains highly proliferative cells from approximately P3 to P10, and it is thought to generate the bulk of granule cells that will reside in the lower GCL (Altman & Bayer, 1990a), adjacent to the hilus.

After the initial formation of the DG, proliferation becomes restricted to the SGZ, the source of newly-generated granule cells that persist throughout adulthood. In Altman and Bayer (1990a), it was suggested that this restriction occurs by P20. Indeed, a more recent and comprehensive study suggested that the SGZ is firmly established by P19 in the rat. They state that “the manner of neurogenesis seen on P19 is nearly identical to that of adult neurogenesis” (Namba et al., 2005, p. 1932). This work extended the original work of Altman and Bayer by also assessing the morphological development of granule neurons using GFP-mediated retroviral labelling. When injected into the developing DG at P5 (the peak of the final stages of initial DG formation from dividing cells in the tertiary matrix) and subsequently analysed at P19, it was found that the majority of labelled cells were present in the GCL and had the critical features of mature granule cells, including a morphological correlate, dendritic spines, and axonal projections to CA3. This suggests that the differentiation of granule neurons from neuroblasts occurs

relatively quickly, and the pattern typically seen in adult neurogenesis is present by approximately P19.

In order to test the hypothesis that the NQZ represents an area of the DG that is the first to undergo age-related declines in neurogenesis, dissociating the initial development of the DG, most of which is postnatal, and the subsequent onset of adult neurogenesis is important. Thus, we have chosen to examine the expansion of the NQZ at ages just beyond the initial formation of the DG. Again, we predicted that the NQZ would not be present immediately after the DG was initially “built”, and would expand its relative size with age, reaching the approximately 1.5% volume fraction we described in Chapter 2 by 3 – 3.5 months of age.

Materials and Methods

Animals

Long-Evans hooded rats were obtained from local breeding stocks in the Department of Neuroscience. Four animals of each of the following ages were used in order to assess the relative size of the NQZ: P21, P25, P35, P60, and ‘adult’ (defined here as 3 – 3.5 months, or P90 – P105).

Perfusions

Perfusions were conducted in a similar manner to those described in Chapter 2. Animals from P21 – P35, however, were perfused using a 60 cc syringe with 35 mL of PBS and 50 mL of 4% PFA. P60 and adult animals were perfused as described in Chapter 2.

Histology

All brains in this study were bisected before cutting frozen microtome sections to allow each hemisphere to be collected independently. In addition, all brains were cut into a ssf of 1/12. Because 12 has multiple factors (6, 4, 3, and 2), this design allowed us to subsequently achieve different ssfs to measure the volume of the GCL and the volume of the GCL associated with the NQZ.

Antibodies

The DCX and GFAP antibodies and dilutions used in the experiments in this chapter were identical to those listed in Table 2 of Chapter 2. The FGF-2 antibody was purchased from Chemicon (catalogue #AB1459) and used at a dilution of 1:2,000.

Immunohistochemistry

The immunohistochemical procedures used in these studies was similar to that described in Chapter 2. For the qualitative analysis of the distribution of FGF-2 in the NQZ, we used ssfs of either 1/3 or 1/4, subsampled from the originally prepared ssf of 1/12.

Cavalieri Volume Estimates

In order to estimate the volume of the GCL and the GCL associated with the NQZ (and thus the volume fraction of the NQZ), we used different ssfs at different ages. This was done under the *a priori* assumption that the NQZ, if present at younger ages, would likely be smaller than that seen in adult animals. Thus, we increased the sampling intensity to a ssf of 1/2 in P21, P25, and P35 animals, but a ssf of 1/3 for P60 and adults. This also allowed us to obtain enough sections through the NQZ to predict the CE. At all ages, a ssf of 1/12 was used to estimate the total GCL volume, as this resulted in only

minor increases in the CE over a ssf of 1/6, and allowed a significant increase in experimental efficiency. Because we determined that the GCL volume and NQZ volume did not exhibit hemispheric asymmetry at any age, we chose series from a single hemisphere of each animal randomly with a probability of 1/2. Thus, all volume estimates reported in this chapter are from single hemispheres.

Given that the noise component of the CE is often the dominant source of error in Cavalieri estimates (Nyengaard, 1999), we also opted to decrease the grid spacing used in our original characterisation of the NQZ (Melvin et al., 2007b) to minimise this contribution. At all ages, the grid size for the total GCL estimates was 0.0064 mm^2 and for the NQZ, 0.0009 mm^2 . All volume estimates were conducted using an automated stereology system from Microbrightfield Biosciences, Inc. (Williston, Vermont) at a magnification of 10x.

Because the ssf of 1/12 provides about 10 sections through the adult DG (and less through younger ages), we used an α value of 12 (corresponding to a smoothness factor of 0) in CE estimates. This same value for α was also used for all NQZ CE calculations as, even at a ssf of 1/3 in adult brain, the mean number of sections obtained was 6. The shape factor employed in total GCL volumes was 18, and 10 for the NQZ.

Statistical analyses of the volume fractions between ages was conducted using a one-way analysis of variance (ANOVA) and Dunnett's *post hoc* procedure using GraphPad Prism 5.01 (La Jolla, California), using the adult group as the control.

Co-localisation of FGF-2 in SGZ Astrocytes

We used confocal microscopy to determine the proportion of FGF-2-expressing GFAP+ astrocytes in the SGZ of 3 – 3.5 month old animals. We defined the SGZ as

extending 3 nuclear diameters below the GCL (Kempermann, 2006). Though practical limitations prevented use visualising DCX under confocal microscopy, these sections were triple-labelled and included DCX labelled with a far red dye (Cy5). In order to discern the boundaries of the NQZ, we confirmed the absences of DCX using epifluorescence microscopy before subsequently obtaining a confocal stack of that region. In the NQZ, we used a ssf of 1/3 and in non-NQZ regions we used a ssf of 1/24. Three fields were randomly sampled on each section using a 60x water immersion lens and a confocal zoom setting of 2.53x. In order to avoid histological confounds associated with damage to the tissue cut surfaces, a subsample of the tissue section height was used for quantification. After finding the middle of the section, the top and bottom of the sampling height was set to 4.0 μm and -4.0 μm , respectively, and z sections spaced 1 μm apart were collected. GFAP+ cell bodies were first identified using a single channel scan and then the FGF-2 signal was revealed to determine co-expression.

Results

The NQZ Volume Fraction Increases with Age

We again made use of the unbiased Cavalieri estimator of volume to quantify the relative size of the NQZ across age. We hypothesized that if the NQZ represents an age-related down-regulation of neurogenesis, then the NQZ volume fraction would become larger over time, reaching the level of $\sim 1.5\%$ at 3 – 3.5 months of age described in our original work (Melvin et al., 2007b).

At both P21 and P25, ages corresponding to the period immediately after the onset of adult SGZ-based neurogenesis (Altman & Bayer, 1990a; Namba et al., 2005), DCX+ cell bodies in the dorsal blade of the anterior pole of the DG are located across its

entire extent (Figure 14 A' shows a P25 animal). Thus, the NQZ does not exist in the early stages of adult neurogenesis. Note that the morphology of DCX+ neuroblasts from the medial region of the dorsal blade (in the area normally occupied by the NQZ in older animals) is typical of that seen in the adult DG, including a relatively thick single dendrite that subsequently bifurcates near the top of the GCL (inset in Figure 14 B'). In P35 animals, however, the NQZ does become apparent (Figure 14 B'), though was obviously smaller than that seen in adult animals.

In order to confirm that the NQZ does expand with age, we subsequently quantified the NQZ volume fraction as a function of age. To accomplish this, we employed the Cavalieri estimator used in our original characterisation of the NQZ (Melvin et al., 2007b; Chapter 2). All values obtained in this chapter are from single hemispheres, as we had previously confirmed that no hemispheric asymmetries existed in either total GCL volume or NQZ volume.

For the NQZ, we used a very intense ssf (1/2) for P21, P25, and P35 under the assumption that, if an NQZ existed at these ages, it would be smaller than that of adult animals. Similarly, a ssf of 1/3 was used for P60 and adult animals in order to reduce the inherent between section variance that resulted from using a ssf of 1/5 or 1/7. This more intense sampling design also enabled us to estimate CEs for the NQZ. The mean absolute volumes of the GCL, the NQZ, and their CEs at different ages are reported in Table 5. Note that the absolute NQZ volume estimate obtained here is 0.019 mm^3 , which is remarkably close to the dual hemisphere estimate of 0.036 mm^3 (which divided by 2 equals 0.018 mm^3) reported in Melvin et al. (2007b; see Chapter 2). We present the critical measures of the NQZ becoming larger relative to the rest of the GCL with age

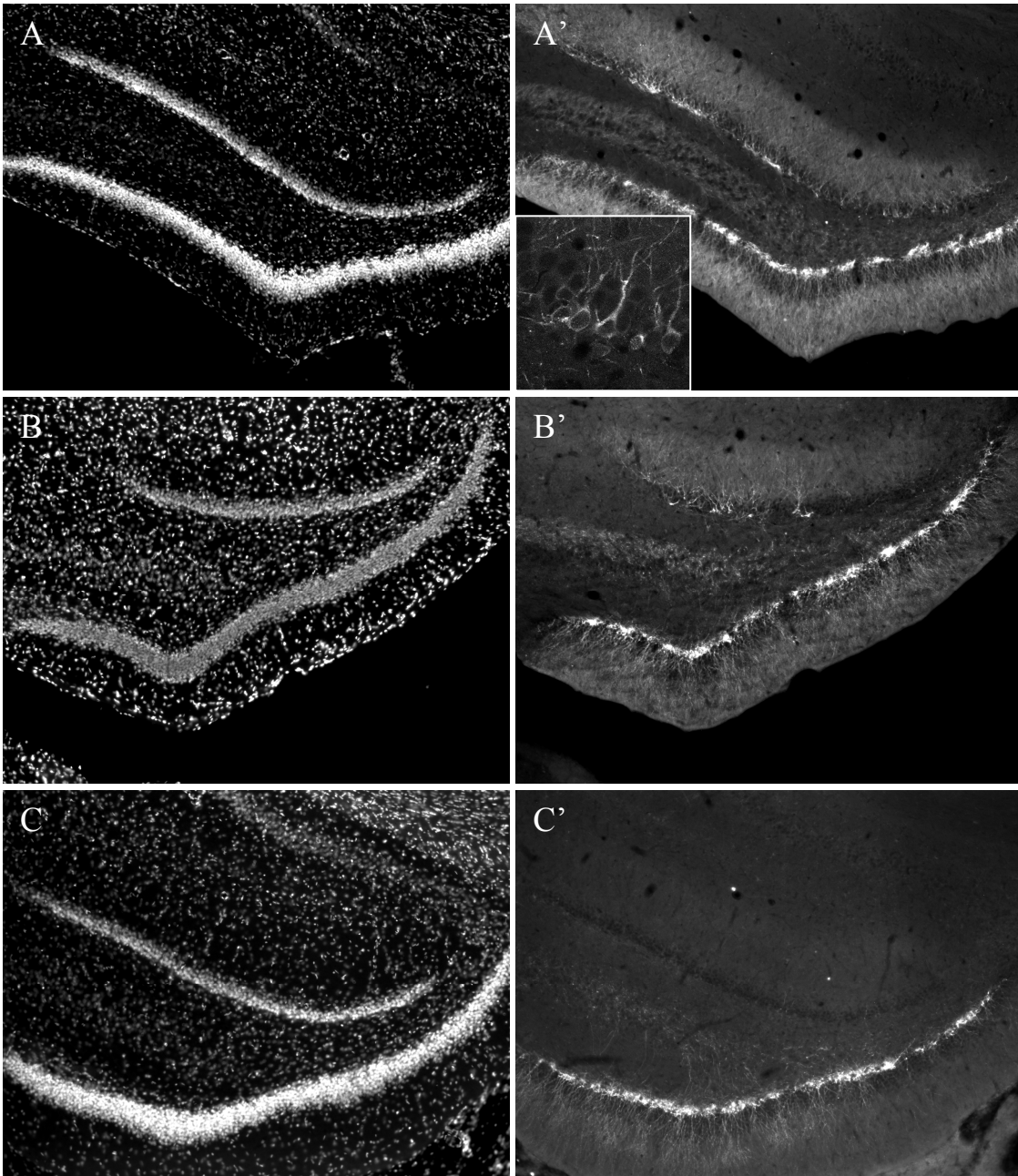


Figure 14. The NQZ is age-dependent. The NQZ does not exist at ages just after the onset of adult neurogenesis (P25, A'). DCX+ cells in the future NQZ have typical morphologies (inset in A'). By P35, the NQZ begins to emerge (B'), and becomes still larger at P60 (C'). A, B, and C are DAPI-labelled images, and A', B', and C' are the corresponding DCX-labelled images.

Table 5

Quantitative estimates of the volume of the granule cell layer (GCL), the neurogenically quiescent zone (NQZ), the NQZ volume fraction, and estimates of precision across age.

Age	mean GCL volume (mm ³)	mean GCL CE	mean NQZ volume (mm ³)	mean NQZ CE
P21	1.028	0.103	0.000	N/A
P25	1.134	0.092	0.000	N/A
P35	1.153	0.075	0.002	0.197
P60	1.164	0.058	0.008	0.113
Adult	1.541	0.060	0.019	0.084

(the NQZ volume fraction) graphically in Figure 15. Note that the NQZ does in fact become increasingly larger with age, consistent with our original prediction of an age-related decline in neurogenesis at the anterior pole of the DG (one-way ANOVA, $F(4, 15) = 133.2$, Dunnett's post test, *** $p < 0.0001$ relative to adult group).

FGF-2 Expression in the NQZ is Qualitatively Similar to non-NQZ Regions

In addition to the age-related increase in the relative size of the NQZ, we also hypothesized that the NQZ in adult animals would be missing specific growth factors that are critical components of the adult neurogenic niche. Our original intention was to assay components of the VEGF, IGF-I, and FGF-2 systems, all of which have been shown to correlate spatially and temporally with decreased DG neurogenesis across age (Shetty et al., 2005). Indeed, the exogenous introduction of these growth factors has been shown to restore levels of neurogenesis in the aged DG to that seen in younger ages (Lichtenwalner et al., 2001; Jin et al., 2003; Shetty et al., 2005; Rai et al., 2007). However, practical limitations prevented much of this work. This issue is discussed in the Discussion section.

Using immunohistochemistry, we mapped the distribution of FGF-2 in the NQZ of adult animals. We found no obvious differences between the density of FGF-2 expressing cells in the NQZ versus non-NQZ regions (Figure 16).

All GFAP+ Astrocytes in the NQZ and non-NQZ Express FGF-2

We and others have reported that the majority of cells in the DG that express FGF-2 are astrocytes (Shetty et al., 2005; Monfils et al., 2006). In the SGZ of 4 month old rats, Shetty et al. (2005) reported that the proportion of GFAP+ astrocytes that co-express FGF-2 is over 90%. By 12 months of age, this decreases to approximately 55%

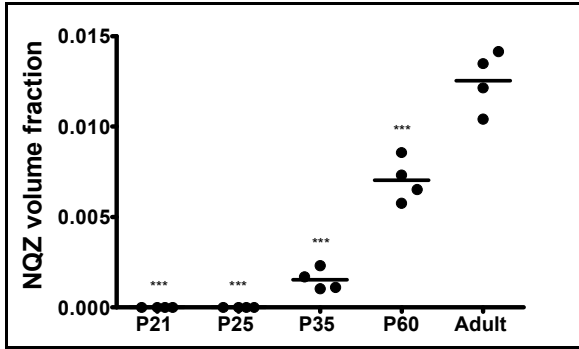


Figure 15. The NQZ expands across age. No NQZ exists early after the onset of adult neurogenesis (P21 and P25), but occupies a progressively larger volume fraction of the DG across age. *** $p < 0.0001$ relative to adults.

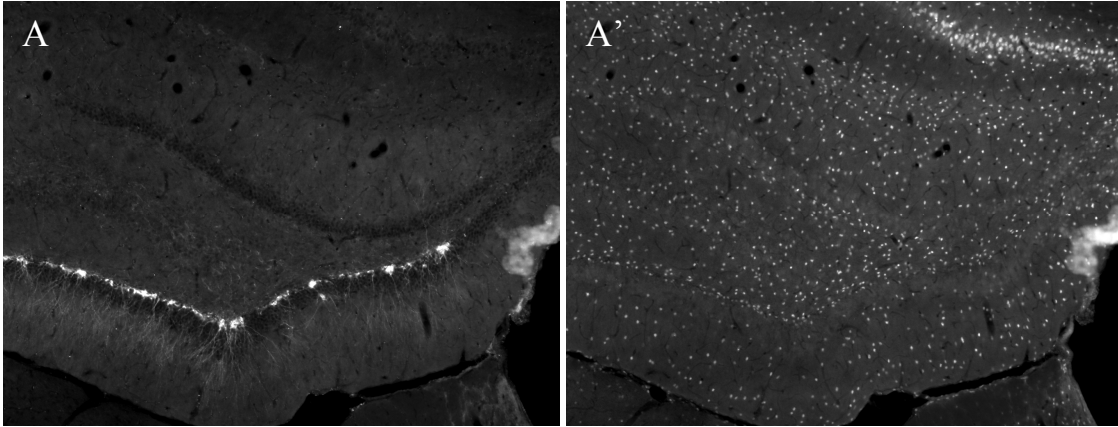


Figure 16. The density of FGF-2 expressing cells is similar in NQZ and non-NQZ regions of the adult DG. DCX immunoreactivity is shown in (A), and FGF-2 immunoreactivity in (A').

and, by 24 months of age, to about 30%. These age-related declines in the SGZ occur despite the persistence of a constant number of GFAP+ astrocytes in the DG up to 24 months. Even though we noted no obvious decline in the density of FGF-2 expressing cells in the NQZ, these results prompted us to look more closely at FGF-2 expression specifically in SGZ astrocytes.

To address this issue, we quantified the proportion of GFAP+ astrocytes in the SGZ in NQZ versus non-NQZ. Remarkably, we found that 100% of SGZ astrocytes expressed FGF-2 in both non-NQZ (Figure 17 A) and NQZ (Figure 17 B) regions. In combination with our qualitative observations on the density of FGF-2 expression, these data suggest that, despite the complete lack of neurogenesis in the NQZ, it exhibits no deficiencies in the local synthesis of this growth factor.

Discussion

The reason why a NQZ exists is perhaps the most interesting question. Unfortunately, this is likely also the most difficult to answer. In an attempt to address this question, we proposed a hypothesis of “early ageing” (Melvin et al., 2007b). This hypothesis is compatible with the possibility that the NQZ lacks neurogenesis because this serves a particular physiological (and possibly behavioural) function. However, addressing the issue of whether the NQZ is physiologically distinct would require precise electrophysiological experiments which were beyond our scope at the time this work was done. However, the critical anatomical data provided in Chapter 2 will be absolutely invaluable to facilitate this approach in the future. Addressing the possibility that the NQZ may contribute a unique function at the behavioural level would also be difficult to determine experimentally. A common approach used in neuroscience to determine how a

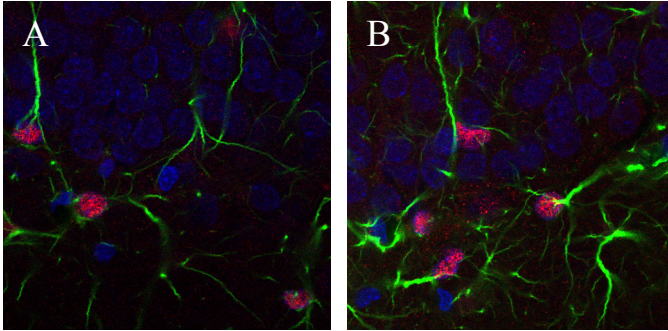


Figure 17. Complete co-expression of FGF-2 in SGZ astrocytes. All GFAP+ astrocytes in the non-NQZ (A) and the NQZ (B) express FGF-2. GFAP+ cells are in green, and FGF-2+ nuclei in red.

particular brain area contributes to behaviour is to selectively lesion the structure in question, and subsequently expose the animal to a variety of behavioural tasks to screen for resulting deficits. However, given the very small size of the NQZ, and its relatively irregular shape, this would be exceedingly difficult. Thus, we chose to focus on the hypothesis that the NQZ represents an area that simply gets old before other areas of the DG.

Our proposal of an “early ageing” hypothesis was based on several similarities between the age-related decreases in DG neurogenesis and the basic characteristics of the NQZ. To begin with, ageing is the most potent endogenous negative regulator of neurogenesis in the DG (Kempermann, 2006). This process is associated not with a decrease in the number of stem cells in the DG across age, but to a dramatic increase in their quiescence (Shetty et al., 2005; Hattiangady & Shetty, 2008). Interestingly, the NQZ, which exists without experimental intervention, has no neurogenesis within the DG of younger animals and the total quiescence of stem cells, despite their presence. Thus, the NQZ may represent an area of the DG that simply undergoes the age-related decline typical of older animals before other areas.

A critical prediction of this hypothesis is that the relative size of the NQZ should increase with age. The data provided in this chapter are consistent with this notion. Though there is no NQZ present at P21 and P25, time points shortly after the last stages of the initial formation of the GCL, the NQZ becomes apparent at P35 and continues to grow in size to adulthood. Whether the NQZ continues to increase in a similar pattern at ages beyond this is not currently known.

Because the emergence of the NQZ occurs soon after the initial development of the DG, one could argue that the lack of an NQZ at P21 and P25 is explained by the time it takes for the last born cells of the tertiary matrix to lose their expression of DCX, and that the NQZ is never capable of supporting adult neurogenesis specifically.

However, several points argue against this conclusion. First, it has been established by previous work that the site of generation of new granule cells in adults, the SGZ, becomes the source of new granule cells by P20 (Altman & Bayer, 1990a).

However, this study assessed the development of the GCL in terms of the location of proliferating cells only. Unfortunately, the time taken for maturing granule cells to lose their expression of DCX during the initial development of the GCL is not known.

However, the study of Namba et al. (2005) assessed the timing of differentiation during development using a GFP-expressing retrovirus. They demonstrated that the morphology typical of mature granule cells, including dendritic spines and axonal projections to CA3 (and thus presumably in their non-DCX-expressing, NeuN-expressing phase) appears by P19. Though this study did not use DCX immunohistochemistry, subsequent studies at both the light (Plumpe et al., 2008) and electron microscopic (Shapiro, Upadhyaya, & Ribak, 2007) level have demonstrated that DCX-expressing neuroblasts in the DG do not have spines, whereas mature granule cells do (Desmond & Levy, 1985). This suggests that the process of neuronal differentiation of cells generated from the tertiary matrix is complete by this age. Thus, it is likely that between the ages of P25 and P35, when the NQZ first appears, is within the early stages of adult neurogenesis.

Further support for our contention that the NQZ initially supports adult neurogenesis, but quickly loses this property, is seen in the progressive increase in the

size of the NQZ at older ages. Even assuming that the differentiation of the last granule cells to be added to the initially developing GCL is not complete by P19, it is unlikely that DCX expression in these cells lasts until the age of P60. However, the NQZ continues to expand after this age, approximately doubling in size during the following month. Taken together, these data support the contention that the NQZ represents a deficit in adult neurogenesis that becomes more pronounced with age.

The original experimental plan to address this hypothesis was much broader than the data in this chapter indicate. Our original intention in testing this hypothesis was to attempt to correlate molecular changes in the NQZ with those known to correlate with the age-related declines in DG neurogenesis, including FGF-2, VEGF, and IGF-I. However, a number of practical limitations prevented much of this work.

We initially wanted to determine whether VEGF and IGF-I exhibited declines in their expression in the NQZ using immunohistochemistry, as we did for FGF-2. However, after trying two independent sources of each antibody with a variety of modifications to our original procedure and the antigen retrieval technique of Eisch (Lagace et al., 2006), we were unsuccessful in all attempts. Indeed, this may be the reason that, in the original study quantifying the age-related declines in FGF-2, VEGF, and IGF-I using enzyme-linked immunosorbent assays, only FGF-2 antibodies were used for immunohistochemistry (Shetty et al., 2005).

We were, however, successful in using one FGF-2 antibody (out of the four different ones purchased for this work) for immunohistochemistry. Our initial experiments indicated that there were no obvious changes in the density of FGF-2+ cells in the NQZ with respect to non-NQZ areas. However, the findings of Shetty et al. (2005)

prompted us to look more closely at FGF-2 with respect to the proportion of astrocytes producing it. In this study, it was reported that over 90% of GFAP+ astrocytes in the SGZ of 4 month old animals express FGF-2. Interestingly, in middle-aged rats, this proportion drops to less than 60% and, in aged rats, to less than 40%. These data are particularly intriguing, given that the exogenous application of FGF-2 can increase DG neurogenesis in aged animals (Rai et al., 2007). As an additional attempt to correlate molecular changes that co-occur in the aged DG with decreased neurogenesis, we examined the proportion of GFAP+ astrocytes in the NQZ and non-NQZ areas in 3 – 3.5 month old animals. Remarkably, in our experiments, we found that every astrocytes in the SGZ of both NQZ and non-NQZ regions expressed FGF-2.

The difference in proportions between our study and that of Shetty et al. (2005) is likely explained by several factors. To begin with, it is possible that there is a decline in FGF-2 synthesis by astrocytes between the ages used in our study (3 months) and the youngest age group used by Shetty et al. (4 months). However, a more likely explanation is differences in our immunohistochemical procedures. We have found that, under “standard” procedures (a 1-2 hour incubation in secondary antibody), essentially no immunohistochemical signal penetrates through the entire depth of the tissue section, and the degree of penetration is highly variable among different antibodies (Melvin & Sutherland, in preparation). Though the incubation time in secondary antibody was not reported in Shetty et al., this group’s previous work always uses a 1 hour incubation in secondary antibody (e.g., Zaman & Shetty, 2003). Finally, differences in the sensitivity of the respective methods also likely differ, as we have noticed dramatically bright signals in immunofluorescence with our extended incubation times. Thus, it is possible that

differential penetration to the tissue core and the less sensitive procedure used by Shetty et al. could account for their report of less than 100% co-expression.

The lack of success of immunohistochemical experiments with VEGF and IGF-I motivated an alternative strategy to determine whether the NQZ was associated with a decrease in expression of these factors. To this end, we attempted to selectively micro-dissect the NQZ from 3 month old animals with the intention of using a polymerase chain reaction (PCR)-based approach. In this strategy, we anaesthetised an animal, quickly removed the unfixed brain, and cut 200 μm thick sections using a vibrotome. Given that the NQZ is present across the entire dorsal blade in anterior coronal sections just before the dorsal and ventral blades meet, we selected sections at this level for our dissection attempts. Using a make-shift tissue punch (a glass capillary tube), we were unsuccessful in obtaining reliable and selective samples of this region with any confidence. Indeed, this is perhaps not surprising when the total volume of the NQZ from Table 4 (0.019 mm^3 in one hemisphere) is converted to a volume measurement more familiar to bench scientists: The total volume of the NQZ is a mere 19 nL. However, given the careful quantitative anatomical characterisation of the NQZ presented in this thesis, the use of laser capture micro-dissection on relatively thick sections through the NQZ would certainly facilitate its selective isolation and ultimate molecular characterisation in comparison to non-NQZ regions.

In this chapter, we provide data that are consistent with an age-related decline in neurogenesis in the NQZ. Though the maintained synthesis of FGF-2 in SGZ astrocytes in the NQZ may seem to argue against this at a mechanistic level, it is possible that the reported decline in FGF-2 synthesis during ageing is merely a correlate of the ageing

process, and not necessarily causal. Indeed, additional correlates, such as declines in the local synthesis of other key niche components, may be shown in future experiments to be the ultimate cause of the lack of neurogenesis in the NQZ. Regardless of the specific mechanisms associated with age-related declines in neurogenesis in the anterior dorsal blade, the data presented here are generally consistent with an age-related decline.

One issue not directly addressed in these studies is that, rather than a lack of permissive factors facilitating neurogenesis, it could also be the case that there is an abundance of an inhibitory factor present in the NQZ. Unfortunately, the identification of endogenous negative regulators of neurogenesis that increase with age has been shown relatively little attention in the literature. However, it is known that elevated levels of glucocorticoids can decrease DG neurogenesis (Cameron & Gould, 1994). Interestingly, the levels glucocorticoids are known to increase during ageing (Sapolsky, 1992). In fact, removing their endogenous source (the adrenal glands) in aged animals restores neurogenesis in the DG (Cameron & McKay, 1999), at least transiently. Thus, it is possible that the local environment in the NQZ is hypersensitive to circulating glucocorticoids relative to non-NQZ areas.

The single factor approaches taken in this chapter further highlight the need for a more comprehensive assay of comparative gene and protein expression in NQZ versus non-NQZ regions. The combination of laser capture micro-dissection to selectively isolate the NQZ with approaches such as microarrays and 2D gel electrophoresis will undoubtedly yield critical information on the molecular mechanisms that mediate neurogenesis in the DG.

CHAPTER FOUR

Neurogenesis can be Behaviourally Induced in the DG

The NQZ constitutively lacks signs of cell divisions and neurogenesis, despite the presence of local stem cells. This implies that the potential exists for this region to support neurogenesis but, under typical laboratory conditions, this potential is not realised. This chapter addresses the following hypothesis: the local stem cells in the NQZ are quiescent but fully capable of adult neurogenesis. This view predicts that neurogenesis can be induced in the NQZ using behavioural treatments known to enhance neurogenesis in the DG. Interestingly, these behavioural paradigms can also increase the levels of neurogenesis in the aged DG (Kronenberg et al., 2006; Segovia, Yague, Garcia-Verdugo, & Mora, 2006).

Of the many events that can induce adult neurogenesis, we chose two behavioural paradigms to test this hypothesis: voluntary exercise (free access to a running wheel) and environmental enrichment. Both treatments have been reported to result in large net increases in neurogenesis, but they appear to do so by acting on different phases of the process, at least under short-term conditions. Wheel running generally increases proliferation in the DG, and environmental enrichment preferentially enhances the survival of newborn neurons, with little or no effect on proliferation (Kempermann et al., 1997; Kronenberg et al., 2003; Olson et al., 2006). Interestingly, longer-term exposure to running wheels resulted in increases in both proliferation and in the number of neuroblasts, but wheel running alone does not result in an ultimate increase in the number of mature granule cells produced (Kronenberg et al., 2006). These findings have led to the suggestion that the relatively “non-specific” effects of physical exercise act to

increase the pool of available progenitors and that more HPC-relevant behavioural challenges like environmental enrichment and learning and memory tasks act to select cells from the expanded pool for survival (Kempermann, 2008).

In this chapter, we describe the results of three independent experiments: Short-term wheel running, longer-term wheel running, and a day-by-day alternating combination of wheel running and environmental enrichment.

Materials and Methods

Animals

All rats were males and 3 – 3.5 months of age at the beginning of each experiment, and were randomly assigned to their respective conditions.

Short-term Wheel Running

In these experiments, all animals were housed in pairs in both control (non-runner) and wheel running conditions. Non-runners were housed in standard laboratory cages. Wheel running cages contained a running wheel attached to a counter, and the distance ran during one 24 period was measured after 3 days of running (3 day runners, $n = 4$) or 7 days of running (7 day runners, $n = 4$) measuring the number of wheel revolutions. Each of the wheel running cages (Mini Mitter, Bend, OR) contained a running wheel (with a diameter of 0.345 m) attached to a counter in order to monitor running activity. The total amount of running is expressed as the distance in meters. Since the circumference of the wheel is the product of the diameter (0.345 m) and π , one revolution is equal to 1.084 m. The total distance ran was therefore the product of 1.084 m and the number of revolutions.

Prior to the first day of running, animals were habituated to this novel environment by exposing them to the cages for 10 minute sessions on 3 consecutive days with the wheel locked to prevent running.

Longer-term Wheel Running

This experiment was conducted in a manner identical to that described for short-term wheel running, with the exception that rats ($n = 4$ in each group) were allowed to run for 14, 20, or 60 days before perfusions.

Alternating Wheel Running and Environmental Enrichment

Rats experienced a 20 day paradigm of alternating wheel running and environmental enrichment. Rats were group housed ($n=6$) in the enriched environment for 24 hours and then were transferred individually to wheel running cages for the subsequent 24 hour period. The enriched environment consisted of a circular tub with a diameter of 1.5 m and height of 60 cm. A wire mesh cover was placed over the top of the tub from which several “bungee cords” were attached. A variety of toys and different lengths of plastic tubing were present in the tub. These components were rearranged every 24 hours in an attempt to encourage exploration.

This experiment was conducted by two other members of our laboratory, Simon Spanswick and Hugo Lehmann, in the context of a different project. The results were reported in Melvin et al. (2007b) with both individuals as co-authors to acknowledge their contribution.

Perfusions

All perfusions were performed as described in previous chapters. In all groups, perfusions took place within 2 hours of the last day of exposure to the respective conditions.

Histology

The brains of rats who experienced the wheel running-only conditions were prepared as described in Chapter 3, bisecting the hemispheres and collecting a ssf of 1/12. Qualitative observations of neurogenesis in the total DG was assessed from a 1/12 ssf, and NQZ qualitative assessments were conducted on a ssf of 1/4.

The brains of rats who experienced the alternating wheel running and environmental enrichment condition were cut, without bisecting, in a ssf of 1/10.

Immunohistochemistry and Imaging

All immunohistochemical and imaging procedures were performed as described in previous chapters.

Results

Wheel Running Alone may not Induce NQZ neurogenesis

Wheel running typically results in a large acute increase in the numbers of cycling cells (van Praag et al., 1999; Kronenberg et al., 2003; Olsen et al., 2006). A study examining the dynamics of this process indicated that the number of proliferating cells peaks between 3 and 10 days after the beginning of wheel running, and declines thereafter despite continued running (Kronenberg et al. 2006). Interestingly, the number of cells expressing markers associated with developing neuroblasts, including DCX, continued to increase. Thus, wheel running results in a significant but transient increase

in the proliferating population of cells in the DG, and differentiation is a slower and cumulative process. We therefore reasoned that, if the NQZ was responsive to wheel running, we would see the appearance of Ki67+ cells in our short-term runners (3 and 7 days), and the appearance of DCX+ neuroblasts in our longer-term runners (14, 20 and 60 day runners).

In contrast to this prediction, we never observed a single Ki67 or DCX+ cell in the NQZ in any running only condition. This may seem to indicate that the NQZ is not responsive to running alone, but our qualitative observations of Ki67 and DCX in non-NQZ regions of these animals revealed no obvious signs of neurogenic induction either, and certainly not the roughly 2-fold increase reported by others (Farmer et al., 2004; Kronenberg et al., 2003; Kronenberg et al., 2006; van Praag et al., 1999). Our observations indicate that, under the conditions used here, wheel running simply did not have a noticeable effect on DG neurogenesis.

The mean distance ran by the 3 day runners and 7 day runners in the short-term condition was 1.26 km and 1.90 km, respectively (the distance ran per day is shown in Figure 18 for each group). In the longer-term running condition, the mean distances ran were 1.10 km, 1.14 km, and 1.70 km for the 14 day runners, 20 day runners, and 60 day runners, respectively (the distance ran per day is shown in Figure 19 for each group). Given that a positive correlation exists between the distance ran and the levels of neurogenesis (Rhodes et al., 2003; Aberg, Perlmann, Olson, & Brene, 2008), the lack of effect seen in our runners is perhaps not surprising. In studies reporting two-fold increases in neurogenesis in rats in response to wheel running, the average distance ran in

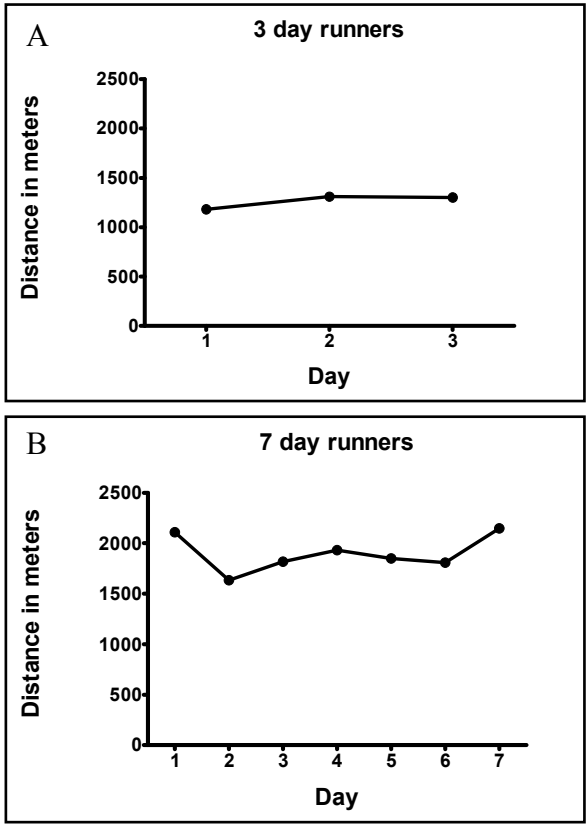


Figure 18. Distance ran per day in short-term runners. In the 3 day runner group, rats ran an average of 1.26 km per day (A), whereas animals in the 7 day runner group ran an average of 1.90 km per day. Each data point represents the average distance ran for 4 animals in two cages.

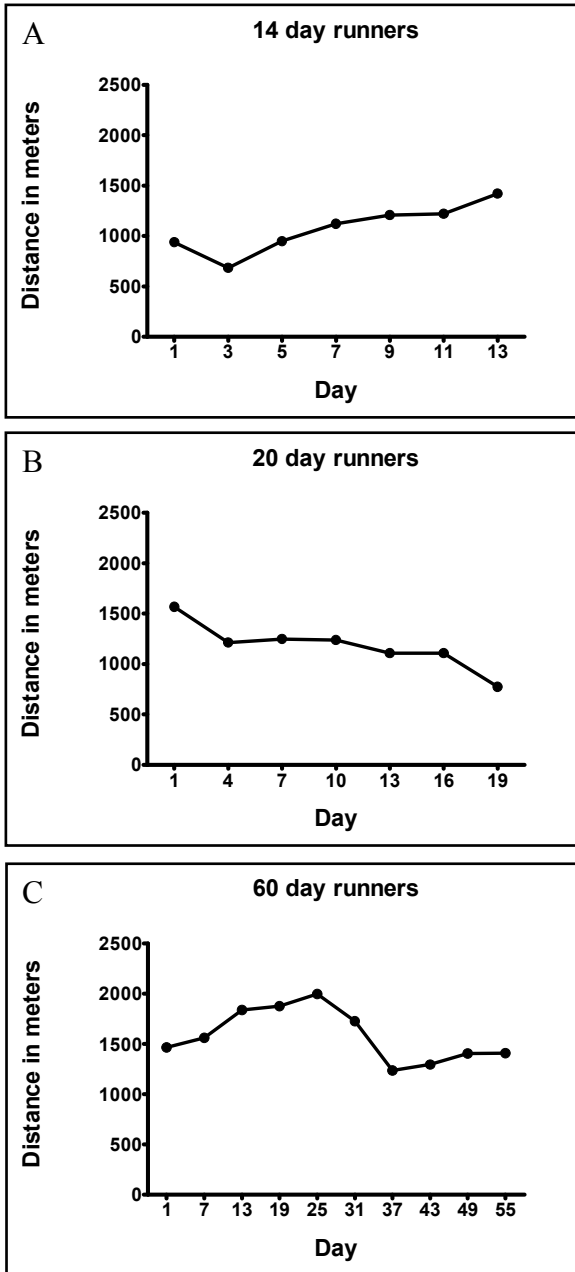


Figure 19. Distance ran per day in longer-term runners. In the 14 day runner group, rats ran an average of 1.10 km per day (A), 20 day runners ran an average of 1.14 km per day (B), and 60 day runners ran an average of 1.70 km per day. Each data point represents the average distance ran for 4 animals in two cages. Data are reported for every second day (A), third day (B), or sixth day (C) for graphical clarity.

animals housed in pairs as in our study was 4.8 km (Farmer et al., 2004), more than two and a half times that seen in our farthest runners.

NQZ Neurogenesis can be Induced Under Some Conditions

In contrast, the alternating wheel running and environmental enrichment paradigm did induce neurogenesis in the NQZ in 5 of the 6 animals (Figure 20). Significantly these DCX+ cells appeared in very anterior sections (Figure 20 A'), well within the presumptive NQZ based on our precise anatomical mapping of its position within the anterior DG. Interestingly, none of the DCX+ cells expressed Ki67 (Figure 20 A''), indicating that, by this point, they were post-mitotic. When viewed at a higher magnification (Figure 20 B), it is apparent that the DCX+ neuroblasts have the morphology typical of neuroblasts in other regions of the adult DG. The tissue from the one animal did not yield any immunohistochemical signal, even to more highly expressed, independent antigens like NeuN. The most likely explanation for this is a non-optimal perfusion.

Discussion

The purpose of the experiments described in this chapter was to determine, qualitatively, whether or not the NQZ is capable of supporting neurogenesis if animals are exposed to behavioural paradigms that have been shown to be potent neurogenic inducers in the DG in general: Wheel running and environmental enrichment. In addition, both of these behavioural conditions are known to increase the levels of neurogenesis in the aged DG (Kronenberg et al., 2006; Segovia et al., 2006).

Typically, wheel running is associated with at least 2-fold increases in neurogenesis (Farmer et al., 2004; Kronenberg et al., 2003; Kronenberg et al., 2006; van

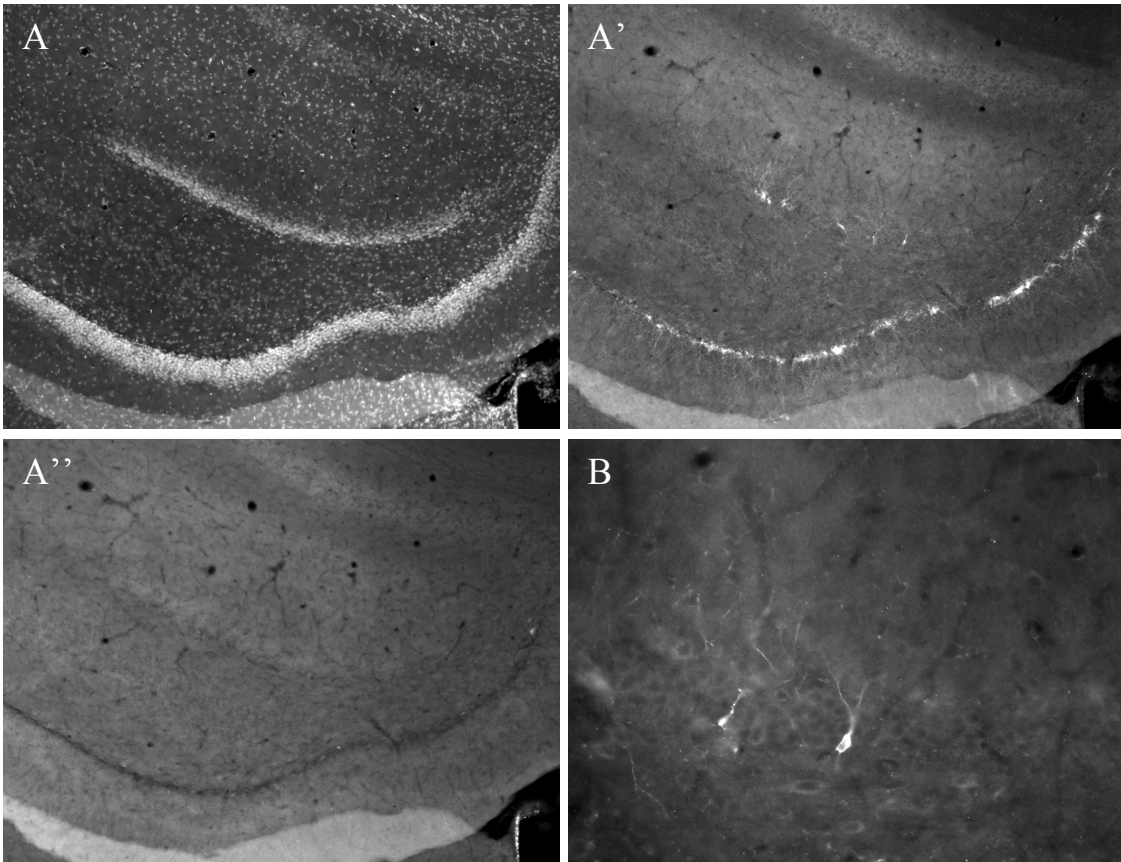


Figure 20. Alternating exposure to wheel running and environmental enrichment induces neurogenesis in the NQZ. The general outline of the GCL is shown with DAPI (A). Note that, although this area of NQZ contains DCX+ neuroblasts (A'), they were never Ki-67+ (A''), indicating that they were post-mitotic by this time point. The image in (B) shows a higher magnification view of the medial-most DCX+ cells shown in (A'). These cells had morphologies typical of neuroblasts in other locations of the DG.

Praag et al., 1999). However, in all of our wheel running alone conditions, we failed to detect any Ki67 or DCX+ cells in the NQZ. Furthermore, we did not detect any visible signs of neurogenesis in the DG in general. The reasons for this are not certain, but the relatively short distance these animals ran is likely to be important. In both short and longer-term running conditions, animals were housed in pairs, which prevented definitively assigning a distance to any individual animal. However, a recent study by Farmer et al. (2004) , in which rats were also housed in pairs with a running wheel, reported that their animals ran an average of 4.8 km per day, more than two and a half times the distance of our farthest runners. Under these conditions, they reported an approximately 2-fold increase in the number of BrdU-labelled cells 4 weeks after multiple daily BrdU injections. In addition, virtually all BrdU-labelled cells expressed the mature neuronal marker NeuN. Though this study did not examine proliferation or differentiation specifically, the presence of 2-fold higher numbers of BrdU cells in the DG suggests that a significant number of cells likely passed through the DCX-expressing neuroblast stage at earlier time points. In a subsequent study, this same group reported a large increase in the number of proliferating BrdU+ cells in running rats 24 hours after injection (Olson et a., 2006). Given the existence of a positive correlation between running distance and the degree of neurogenesis (Rhodes et al., 2003; Aberg et al., 2008), it is perhaps not surprising that we failed to see any obvious signs of neurogenic induction. Thus, the lack of any observable increase in either cell proliferation or the number of neuroblasts in the DG as a whole is likely explained by the fact that our neurogenic effect was simply not strong enough.

In contrast, we did detect the presence of DCX+ neuroblasts in the NQZ after a 20 day alternating wheel running and environmental enrichment paradigm. The mean running distance for these animals, which were housed alone with a running wheel, was 1.26 km. Assuming that each animal had equal access to the running wheel in our short and longer-term running only experiments (where they were housed in pairs), these distances represent approximately half that seen in the alternating paradigm. Thus, it is possible that the increased running intensity seen in the alternating paradigm resulted in a sufficiently strong stimulus to cause increases in the proliferative pool of cells (as previously reported in several studies), and the intervening days of environmental enrichment favoured their subsequent survival and differentiation to the DCX-expressing stage. However, because the alternating exposure experiment did not include a 20 day running only condition, it is not possible to discern whether the appearance of neuroblasts in the NQZ under these conditions was due to exercise intensity or to the synergistic effects of wheel running and environmental enrichment. Regardless of the specific cause, it is clear from our studies is that the NQZ is in fact capable of supporting local neurogenesis in response to some behavioural challenges, but not others.

The molecular effects that mediate the increase in neurogenesis after wheel running and environmental enrichment appear to be mediated by a large number of signalling molecules (Olson et al., 2006). However, the key changes under both conditions appear to be increases in the levels of a variety of growth factors. FGF-2, brain-derived neurotrophic factor, IGF-I and VEGF are all increased after exercise and, for IGF-I and VEGF, their subsequent peripheral blockade largely prevents increases in exercise-induced neurogenesis (Gomez-Pinilla et al., 1997; Trejo et al., 2001; Fabel et al.,

2003). Environmental enrichment also results in increases in key growth factors, including VEGF (Cao et al., 2004) and a number of members of the neurotrophin family (Olson et al., 2006).

Though the levels of growth factors present in the NQZ after 20 days of alternating wheel running and environmental enrichment were not assayed in these studies, it is likely that increases in several of the growth factors discussed above may have accounted for this effect. However, to our knowledge, a daily alternating paradigm of wheel running and environmental enrichment has never been conducted, and it is not necessarily easy to predict which growth factors may have been induced or their temporal expression patterns from the known effects of wheel running and enrichment alone. Certainly, determining the molecular changes in NQZ's local niche would be a monumental task using the single or limited multi-factor approaches (immunohistochemistry and related techniques) typically used. A more comprehensive alternating paradigm design, complete with yoked single paradigm exposure controls and in combination with the selective isolation of the NQZ with laser capture micro-dissection and high-throughput gene expression assays, would allow the molecular changes in the NQZ to be assessed.

The effects of environmental enrichment and wheel running include complex physical and cognitive elements. It is beyond the scope of this work to tease these elements apart. However, the purpose of these experiments was simply to determine, from a qualitative perspective, if the NQZ was capable of supporting neurogenesis under behavioural conditions known to increase DG neurogenesis in general. Despite the

complexities involved, we have determined that, under the circumstances tested here, neurogenesis can be induced in the NQZ, albeit at low levels.

CHAPTER FIVE

Potential Reasons for the Existence of the NQZ

This thesis describes and characterises a novel area of the adult rat DG that constitutively lacks neurogenesis. As discussed previously, the reasons for the existence of the NQZ can be analyzed at multiple levels. Based on the existing literature and the work presented here, we suggest that the most parsimonious explanation at a cellular and molecular level is that the NQZ lacks critical niche factors that normally facilitate neurogenesis, and that the NQZ may represent an area of the DG that succumbs to the age-related declines before other areas.

Several findings from this thesis are consistent with this hypothesis. To begin with, ageing is associated with strong decreases in the levels of neurogenesis, beginning its decline at a relatively young age (Shetty et al., 2005). We present data that suggest that, initially after the formation of the DG, the area associated with the NQZ is capable of supporting neurogenesis, but subsequently becomes non-neurogenic. As predicted from an age-related hypothesis, the NQZ continues to expand across time.

Curiously, the general decline in DG neurogenesis with age is not associated with a decrease in the number of stem cells available to generate new neurons, but an increase in the degree of stem cell quiescence (Hattiangady & Shetty, 2008). This phenotype is temporally and spatially associated with the decreased expression of a number of growth factors known to be pro-neurogenic, such as FGF-2, IGF-I, and VEGF (Shetty et al., 2005). The fact that the NQZ is capable of neurogenesis in response to treatments that are known to induce the expression of these and other growth factors (Olson et al., 2006) provides further support for this contention.

Given that the NQZ contains stem cells that are, by definition, quiescent, it is interesting to speculate that the missing niche factors are those that are associated normally with an actively cycling population of stem cells. We were unable to assess the molecular changes that occur in this region of the DG under basal and induced conditions, but we believe our data demonstrating the presence of a non-cycling stem cell population, the increase in the size of the NQZ with age, and the fact that behavioural treatments that have been shown to increase neurogenesis in aged rodents (Kempermann et al., 2002; Segovia et al., 2006; Kronenberg et al., 2006) can induce neurogenesis in the NQZ provide reasonable cause to pursue this hypothesis.

The possibility that the NQZ represents a region of the adult DG whose function depends on the absence of neurogenesis cannot be excluded. Unfortunately, testing this hypothesis with the methods often employed in neuroscience, for example permanent or temporary inactivations, cannot be readily applied, given the small size and irregular shape of the NQZ. However, insights could be gained by determining whether this region exhibits special electrophysiological correlates during a variety of HPC-dependent behavioural tasks.

It is possible that, rather than being viewed as a deficiency, the lack of basal neurogenesis in the NQZ may represent a useful physiological adaptation. One consequence of the addition of new neurons to the DG is an increase in electrical excitability, including a reduced threshold for the induction of long-term potentiation (Farmer et al., 2004; Schmidt-Hieber et al., 2004; Wang et al., 2000). DG long-term potentiation, in contrast to other regions of the HPC, is associated with excessive glutamate accumulation (Errington, Galley, & Bliss, 2003), and excess glutamate

accumulation is associated with the generation of seizure activity (Urbanska, Czuczwar, Kleinrik, & Turski, 1998). Though purely speculative, it is possible that the lack of neurogenesis in the NQZ serves to prevent this area from becoming epileptogenic.

The Utility of the NQZ

The existence of ongoing neurogenesis in adult brains has stimulated a wealth of research into its mechanisms. Though admittedly an over-simplification, much of the knowledge gained in this field comes from experiments designed in a conceptually similar format: Apply a treatment (for example, a drug or exogenous growth factor), induce a disease condition, or expose animals to a behavioural paradigm, and assess whether the levels of neurogenesis by a variety of measures have been modulated. Subsequently, signs of molecular changes are then often searched for using single factor or limited multi-factor approaches to detect changes in the levels or functioning of suspected molecules that might play a role in the phenomenon under study.

The use of high-throughput, global measures of changes in gene expression (as opposed to single or limited multi-factor approaches) have made fundamental contributions to several areas of biology and medicine (Weston & Hood, 2004). The use of a variety of techniques to compare gene expression between two tissue types at the level of transcripts (referred to collectively here as “transcriptomics”) and at the level of proteins (“proteomics”) offer the ability to uncover molecular differences *en masse*.

These experimental approaches have been applied in different contexts to study the processes associated with neurogenesis. For example, two studies have used SVZ-derived neurospheres to determine the changes that occur at the transcript level during differentiation induced by the removal of growth factors from the culture medium

(Bonnert et al., 2006; Gurok et al. 2004). Conceptually similar approaches using embryonic stem cells subjected to proteomic analysis have also been used (Akama et al., 2008). However, because of the powerful regulatory influences of the local cellular environment in creating the neurogenic niche, such *in vitro* preparations are likely to have limited *in vivo* relevance.

In an effort to study the mechanisms of cell proliferation in the DG, Gurok et al. (2007) administered electroconvulsive shock treatments to adult rats, a potent inducer of proliferation in the adult DG (Wennstrom, Hellsten, Ekdahl & Tingstrom, 2003). Transcripts from shocked versus a non-shocked reference were then compared using microarrays. The limitation of studies like these is that they use experimentally-induced conditions (i.e., seizures) in order to accentuate the process of interest. The possibility exists that the induction of cell proliferation under these conditions may not engage the same mechanisms that occur under basal conditions.

Ideally, the discovery of the molecular regulators of neurogenesis with maximal efficiency and *in vivo* relevance would require an amenable model system with the following characteristics. First, the availability of a target tissue that exhibits very similar phenotypic properties to another “control” or reference tissue, but differs only with respect to the processes of interest, would provide valuable starting material. Second, in order to minimize potentially confounding variables, the target tissue should exhibit the critical phenotypic differences under “natural” (defined here solely as “without experimental induction”) conditions. Third, the target tissue should be readily identifiable between different animals, with its location well mapped qualitatively and quantitatively. This would facilitate the selective isolation and pooling of tissues from different animals

if the target tissue volume is prohibitively small to use as starting material for proteomic or transcriptomic work. Fourth, ideally both the target and reference tissues should exist within a single animal, eliminating or at least drastically reducing the between-animal variability that can be a significant source of noise in these assays.

This thesis reports the discovery and characterisation of a discrete area of the DG that constitutively lacks neurogenesis under basal conditions. The NQZ is present in the dorsal blade of the anterior pole of the adult rat DG. This area is remarkably similar to other areas of the DG that do undergo constitutive neurogenesis. Specifically, it contains several elements of the local niche, including mature neurons and glia, blood vessels, and the growth factor FGF-2. Despite lacking ongoing neurogenesis under basal conditions, the NQZ does contain stem cells but, given the total absence of cell proliferation in this area, they are mitotically quiescent. These factors are similar to those in age-related declines in neurogenesis in rodents (Hattiangady & Shetty, 2008; Rao et al., 2006). However, neurogenesis can be induced in the NQZ by some behavioural paradigms. Finally, we have used a stereological approach with high precision to map the size and location of the NQZ, which exhibits remarkable similarities between animals. We believe that these properties make the NQZ the best currently available model system with which to discern the mechanisms of adult neurogenesis.

One aspect of the original experimental plan for our studies was to compare differential gene expression between the NQZ and non-NQZ regions from individual animals using microarrays. Since these two regions appear very similar in several basic respects except with regards to the process of neurogenesis, such an analysis would in principle identify the molecular regulators that facilitate basal neurogenesis in the adult

DG. Unfortunately, technical limitations prevented this work from advancing. Notably, the extremely small size of the NQZ (~ 19 nL in one hemisphere) made its selective isolation via manual dissection impossible. Fortunately, the NQZ can be identified using anatomical landmarks: It is present across the entire dorsal blade of the DG at positions before the dorsal and ventral blades meet at the apex. Thus, the NQZ is an ideal candidate for the use of specialized dissection techniques such as laser capture micro-dissection.

In order to be of use in measures of differential gene expression, obtaining a pure NQZ sample, without contamination from non-NQZ regions, would be critical to the success of such comparisons. Since the NQZ is defined by the absence of DCX protein expressing cell bodies, and the DCX transcript is restricted to cell bodies *in vivo* (Dr. Carola Haas, personal communication), sample purity could be confirmed by using reverse transcriptase-polymerase chain reaction with DCX-specific primers. Given that the expression of DCX is essentially “shoulder to shoulder” in non-NQZ regions, contamination of NQZ isolates by adjacent non-NQZ can be monitored.

The choice between a proteomics approach or a transcript-based assay like microarrays can be assessed by considering their relative advantages and disadvantages. Given the small volume occupied by the NQZ, tissue samples from any one animal will provide limited quantities of starting material. In this light, nucleic acid-based strategies offer a significant advantage because the samples can be amplified (Singh et al., 2004). Given the phenotypic similarities between the NQZ and non-NQZ regions, it is likely that such an analysis will provide a relatively manageable list of differentially expressed genes relevant to neurogenesis. Indeed, this type of expression profiling has been used successfully to differentiate previously homogeneously-grouped cancers into distinct

molecular subtypes (Golub et al., 1999). With regard to neurogenesis, one group has recently published a custom array called the “NeuroStem Chip” (Anisimov, Christophersen, Correia, Li, & Brundin, 2007), which contains 1,300 genes involved in various stages of the process of neurogenesis. Subjecting the NQZ to this type of analysis would likely provide a wealth of preliminary information, possibly identifying the lack of permissive factors or the presence of inhibitory factors that prevent neurogenesis.

Despite the analytical power of microarrays, the real “molecular workhorses” of the cell are proteins. Therefore, assessing changes solely at the transcriptional level provides limited information regarding the functional state of cells within a given tissue. A great deal of the molecular diversity is conferred on cells at the level of proteins, which would not be detectable with nucleic acid-based strategies (Primrose & Twyman, 2006). Given these limitations, a proteomics-based approach to assessing differential gene expression would yield more detailed information regarding the functional differences between NQZ and non-NQZ areas. However, these methods have limitations of their own, which are significant in the context of the NQZ. Because protein samples cannot be amplified like nucleic acids, and the detection techniques in proteomics are less sensitive, a relatively large amount of starting material is required. Therefore, a single sample from the NQZ of a single animal will not produce sufficient material for a successful analysis of local proteome. One aspect of the NQZ discovered in our studies is the remarkable similarity of the size and positions of the NQZ between animals. Thus, samples from multiple animals could likely be pooled to facilitate these experiments.

Undoubtedly, discovering the genes and gene products involved in the process of DG neurogenesis will have far reaching consequences. Not only will such studies reveal

the molecular mechanisms that allow this process to occur, but they will also likely contribute key information with regard to how this process may relate to the functional role that ongoing neurogenesis plays in the DG.

REFERENCES

- Aberg, M.A., Aberg, N.D., Hedbacker, H., Oscarsson, J., & Eriksson, P.S. (2000). Peripheral infusion of IGF-I selectively induces neurogenesis in the adult rat hippocampus. *The Journal of Neuroscience*, *20*, 2896-2903.
- Aberg, E., Perlmann, T., Olson, L., & Brene, S. (2008). Running increases neurogenesis without retinoic acid receptor activation in the adult mouse dentate gyrus. *Hippocampus*, *18*, 785-792.
- Abrous, D.N., Koehl, M., & Le Moal, M. (2005). Adult neurogenesis: from precursors to network and physiology. *Physiological Reviews*, *85*, 523-569.
- Aimone, J.B., Wiles, J., & Gage, F.H. (2006). Potential role for adult neurogenesis in the encoding of time in new memories. *Nature Neuroscience*, *9*, 723-727.
- Akama, K., Tatsuno, R., Otsu, M., Horikoshi, T., Nakayama, T., Nakamura, M., Toda, T., & Inoue, N. (2008). Proteomic identification of differentially expressed genes in mouse neural stem cells and neurons differentiated from embryonic stem cells in vitro. *Biochimical et Biophysical Acta*, *1784*, 773-782.
- Altman, J., & Bayer, S.A. (1990a). Migration and distribution of two populations of hippocampal granule cell precursors during the perinatal and postnatal periods. *The Journal of Comparative Neurology*, *301*, 365-381.
- Altman, J., & Bayer, S.A. (1990b). Mosaic organization of the hippocampal neuroepithelium and the multiple germinal sources of dentate granule cells. *The Journal of Comparative Neurology*, *301*, 325-342.

- Alvarez-Buylla, A., Garcia-Verdugo, J.M., & Tramontin, A.D. (2001). A unified hypothesis on the lineage of neural stem cells. *Nature Reviews Neuroscience*, 2, 287-293.
- Amaral, D., & Lavenex, P. (2007). Hippocampal neuroanatomy. In P. Andersen, R. Morris, D. Amaral, T. Bliss, & J. O'Keefe (Eds.), *The hippocampus book* (pp. 37-114). New York, NY: Oxford University Press.
- Anisimov, S.V., Christophersen, N.S., Correia, A.S., Li, J.Y., & Brundin, P. (2007). "NeuroStem Chip": a novel highly specialized tool to study neural differentiation pathways in human stem cells. *BioMed Central Genomics*, 8, 1-15.
- Babu, H., Cheung, G., Kettenmann, H., Palmer, T.D., & Kempermann, G. (2007). Enriched monolayer precursor cell cultures from micro-dissected adult mouse dentate gyrus yield functional granule cell-like neurons. *Public Library of Science One*, 2, e388.
- Banasr, M., Soumier, A., Hery, M., Mocaer, E., & Daszuta, A. (2006). Agomelatine, a new antidepressant, induces regional changes in hippocampal neurogenesis. *Biological Psychiatry*, 59, 1087-1096.
- Bermejo, P.E., Jimenez, C.E., Torres, C.V., & Avendano, C. (2003). Quantitative stereological evaluation of the gracile and cuneate nuclei and their projection neurons in the rat. *The Journal of Comparative Neurology*, 463, 419-433.
- Bonnert, T.P., Bilsland, J.G., Guest, P.C., Heavens, R., McLaren, D., Dale, C., Thakur, M., McAllister, G., & Munoz-Sanjuan, I. (2006). Molecular characterization of adult mouse subventricular zone progenitor cells during the onset of differentiation. *The European Journal of Neuroscience*, 24, 661-675.

- Brown, J.P., Couillard-Despres, S., Cooper-Kuhn, C.M., Winkler, J., Aigner, L., & Kuhn, H.G. (2003). Transient expression of doublecortin during adult neurogenesis. *The Journal of Comparative Neurology*, 467, 1-10.
- Burwell, R.D., & Amaral, D.G. (1998). Perirhinal and postrhinal cortices of the rat: interconnectivity and connections with the entorhinal cortex. *The Journal of Comparative Neurology*, 391, 293-321.
- Cameron, H.A., & Gould, E. (1994). Adult neurogenesis is regulated by adrenal steroids in the dentate gyrus. *Neuroscience*, 61, 203-209.
- Cameron, H.A., & McKay, R.D. (1999). Restoring production of hippocampal neurons in old age. *Nature Neuroscience*, 2, 894-897.
- Campuzano, R., Barrios, V., Cuevas, B., Asín-Cardiel, E., Muela, A., Castro, J.M., Fernandez-Ayerdi, A., & Cuevas, P. (2002). Serum basic fibroblast growth factor levels in exercise-induced myocardial ischemia more likely a marker of endothelial dysfunction than a marker of ischemia?. *European Journal of Medical Research*, 7, 93-97.
- Cao, L., Jiao, X., Zuzga, D.S., Liu, Y., Fong, D.M., Young, D., & During, M.J. (2004). VEGF links hippocampal activity with neurogenesis, learning and memory. *Nature Genetics*, 36, 827-835.
- Carlson, M.E., & Conboy, I.M. (2007). Regulating the Notch pathway in embryonic, adult and old stem cells. *Current Opinion in Pharmacology*, 7, 303-309.
- Cebe-Suarez, S., Zehnder-Fjallman, A., & Ballmer-Hofer, K. (2006). The role of VEGF receptors in angiogenesis; complex partnerships. *Cellular and Molecular Life Sciences*, 63, 601-615.

- Chen, H., Tung, Y.C., Li, B., Iqbal, K., & Grundke-Iqbal, I. (2007). Trophic factors counteract elevated FGF-2-induced inhibition of adult neurogenesis. *Neurobiology of Aging*, *28*, 1148-1162.
- Cheng, Y., Black, I.B., & DiCicco-Bloom, E. (2002). Hippocampal granule neuron production and population size are regulated by levels of bFGF. *The European Journal of Neuroscience*, *15*, 3-12.
- Coller, H.A., Sang, L., & Roberts, J.M. (2006). A new description of cellular quiescence. *Public Library of Science Biology*, *4*, e83.
- Cruz-Orive, L.M., Insausti, A.M., Insausti, R., & Crespo, D. (2004). A case study from neuroscience involving stereology and multivariate analysis. In S.M. Evans, A.M. Janson, & J.R. Nyengaard (Eds.), *Quantitative methods in neuroscience* (pp. 16-64). Oxford, England: Oxford University Press.
- Desmond, N.L., & Levy, W.B. (1985). Granule cell dendritic spine density in the rat hippocampus varies with spine shape and location. *Neuroscience Letters*, *54*, 219-224.
- Doetsch, F., Caille, I., Lim, D.A., García-Verdugo, J.M., & Alvarez-Buylla, A. (1999). Subventricular zone astrocytes are neural stem cells in the adult mammalian brain. *Cell*, *97*, 703-716.
- Duijvestijn, A.M., van Goor, H., Klatter, F., Majoor, G.D., van Bussel, E., & van Breda Vriesman, P.J. (1992). Antibodies defining rat endothelial cells: RECA-1, a pan-endothelial cell-specific monoclonal antibody. *Laboratory Investigation*, *66*, 459-466.

- Eisch, A.J., & Mandyam, C.D. (2007). Adult neurogenesis: can analysis of cell cycle proteins move us "Beyond BrdU"? *Current Pharmaceutical Biotechnology*, 8, 147-165.
- Endl, E., & Gerdes, J. (2000). The Ki-67 protein: fascinating forms and an unknown function. *Experimental Cell Research*, 257, 231-237.
- Errington, M.L., Galley, P.T., & Bliss, T.V. (2003). Long-term potentiation in the dentate gyrus of the anaesthetized rat is accompanied by an increase in extracellular glutamate: real-time measurements using a novel dialysis electrode. *Philosophical Transactions of the Royal Society of London. Series B, Biological Sciences*, 358, 675-687.
- Fabel, K., Fabel, K., Tam, B., Kaufer, D., Baiker, A., Simmons, N., Kuo, C.J., & Palmer, T.D. (2003). VEGF is necessary for exercise-induced adult hippocampal neurogenesis. *The European Journal of Neuroscience*, 18, 2803-2812.
- Farmer, J., Zhao, X., van Praag, H., Wodtke, K., Gage, F.H., & Christie, B.R. (2004). Effects of voluntary exercise on synaptic plasticity and gene expression in the dentate gyrus of adult male Sprague-Dawley rats in vivo. *Neuroscience*, 124, 71-79.
- Ferri, A.L., Cavallaro, M., Braidà, D., Di Cristofano, A., Canta, A., Vezzani, A., Ottolenghi, S., Pandolfi, P.P., Sala, M., DeBiasi, S., & Nicolis, S.K. (2004). Sox2 deficiency causes neurodegeneration and impaired neurogenesis in the adult mouse brain. *Development*, 131, 3805-3819.

- Filippov, V., Kronenberg, G., Pivneva, T., Reuter, K., Steiner, B., Wang, L.P., Yamaguchi, M., Kettenmann, H., & Kempermann, G. (2003). Subpopulation of nestin-expressing progenitor cells in the adult murine hippocampus shows electrophysiological and morphological characteristics of astrocytes. *Molecular and Cellular Neurosciences*, 23, 373-382.
- Fong, H., Hohenstein, K.A., & Donovan, P.J. (2008). Regulation of Self-renewal and Pluripotency by Sox2 in Human Embryonic Stem Cells. *Stem Cells*, 26, 1931-1938.
- Fukuda, S., Kato, F., Tozuka, Y., Yamaguchi, M., Miyamoto, Y., & Hisatsune, T. (2003). Two distinct subpopulations of nestin-positive cells in adult mouse dentate gyrus. *The Journal of Neuroscience*, 23, 9357-9366.
- Gage, F.H., Coates, P.W., Palmer, T.D., Kuhn, H.G., Fisher, L.J., Suhonen, J.O., Peterson, D.A., Suhr, S.T., & Ray, J. (1995). Survival and differentiation of adult neuronal progenitor cells transplanted to the adult brain. *Proceedings of the National Academy of Sciences of the United States of America*, 92, 11879-11883.
- Garcia, A.D., Doan, N.B., Imura, T., Bush, T.G., & Sofroniew, M.V. (2004). GFAP-expressing progenitors are the principal source of constitutive neurogenesis in adult mouse forebrain. *Nature Neuroscience*, 7, 1233-1241.
- Givogri, M.I., de Planell, M., Galbiati, F., Superchi, D., Gritti, A., Vescovi, A., de Vellis, J., & Bongarzone, E.R. (2006). Notch signaling in astrocytes and neuroblasts of the adult subventricular zone in health and after cortical injury. *Developmental Neuroscience*, 28, 81-91.

- Golub, T.R., Slonim, D.K., Tamayo, P., Huard, C., Gaasenbeek, M., Mesirov, J.P., Coller, H., Loh, M.L., Downing, J.R., Caligiuri, M.A., Bloomfield, C.D., & Lander, E.S. (1999). Molecular classification of cancer: class discovery and class prediction by gene expression monitoring. *Science*, 286, 531-537.
- Gomez-Pinilla, F., Dao, L., & So, V. (1997). Physical exercise induces FGF-2 and its mRNA in the hippocampus. *Brain Research*, 764, 1-8.
- Green, E.J., & Juraska, J.M. (1985). The dendritic morphology of hippocampal dentate granule cells varies with their position in the granule cell layer: a quantitative Golgi study. *Experimental Brain Research*, 59, 582-586.
- Gundersen, H.J., & Jensen, E.B. (1987). The efficiency of systematic sampling in stereology and its prediction. *Journal of Microscopy*, 147, 229-263.
- Gundersen, H.J., Jensen, E.B., Kiêu, K., & Nielsen, J. (1999). The efficiency of systematic sampling in stereology--reconsidered. *Journal of Microscopy*, 193, 199-211.
- Gurok, U., Steinhoff, C., Lipkowitz, B., Ropers, H.H., Scharff, C., & Nuber, U.A. (2004). Gene expression changes in the course of neural progenitor cell differentiation. *The Journal of Neuroscience*, 24, 5982-6002.
- Gurok, U., Loebbert, R.W., Meyer, A.H., Mueller, R., Schoemaker, H., Gross, G., & Behl, B. (2007). Laser capture microdissection and microarray analysis of dividing neural progenitor cells from the adult rat hippocampus. *The European Journal of Neuroscience*, 26, 1079-1090.
- Hagg T. (2005). Molecular regulation of adult CNS neurogenesis: an integrated view. *Trends in Neurosciences*, 28, 589-595.

- Hattiangady, B., & Shetty, A.K. (2008). Aging does not alter the number or phenotype of putative stem/progenitor cells in the neurogenic region of the hippocampus. *Neurobiology of Aging*, *29*, 129-147.
- Hirao, A., Arai, F., & Suda, T. (2004). Regulation of cell cycle in hematopoietic stem cells by the niche. *Cell Cycle*, *3*, 1481-1483.
- Howard, C.V., & Reed, M.G. (2005). *Unbiased stereology* (2nd ed.). New York, NY: BIOS Scientific Publishers.
- Ihrie, R.A., & Alvarez-Buylla, A. (2008). Cells in the astroglial lineage are neural stem cells. *Cell Tissue Research*, *331*, 179-191.
- Jalava, N.S., Lopez-Picon, F.R., Kukko-Lukjanov, T.K., & Holopainen, I.E. (2007). Changes in microtubule-associated protein-2 (MAP2) expression during development and after status epilepticus in the immature rat hippocampus. *International Journal of Developmental Neuroscience*, *25*, 121-131.
- Jayatissa, M.N., Bisgaard, C., Tingstrom, A., Papp, M., & Wiborg, O. (2006). Hippocampal cytogenesis correlates to escitalopram-mediated recovery in a chronic mild stress rat model of depression. *Neuropsychopharmacology*, *31*, 2395-2404.
- Jin, K., Zhu, Y., Sun, Y., Mao, X.O, Xie, L., & Greenberg, D.A. (2002). Vascular endothelial growth factor (VEGF) stimulates neurogenesis in vitro and in vivo. *Proceedings of the National Academy of Sciences of the United States of America*, *99*, 11946-11950.

- Jin, K., Sun, Y., Xie, L., Batteur, S., Mao, X.O., Smelick, C., Logvinova, A., & Greenberg, D.A. (2003). Neurogenesis and aging: FGF-2 and HB-EGF restore neurogenesis in hippocampus and subventricular zone of aged mice. *Aging Cell*, 2, 175-183.
- Kempermann, G. (2006). *Adult neurogenesis*. Oxford, England: Oxford University Press.
- Kempermann, G. (2006). They are not too excited: the possible role of adult-born neurons in epilepsy. *Neuron*, 52, 935-937.
- Kempermann, G. (2008). Activity dependency and aging in the regulation of adult neurogenesis. In F.H. Gage, G. Kempermann, & H. Song (Eds.), *Adult neurogenesis* (pp. 341-362). New York, NY: Cold Spring Harbor Laboratory Press.
- Kempermann, G., Gast, D., & Gage, F.H. (2002). Neuroplasticity in old age: sustained fivefold induction of hippocampal neurogenesis by long-term environmental enrichment. *Annals of Neurology*, 52, 135-143.
- Kempermann, G., Gast, D., Kronenberg, G., Yamaguchi, M., Gage, F.H. (2003). Early determination and long-term persistence of adult-generated new neurons in the hippocampus of mice. *Development*, 130, 391-399.
- Kempermann, G., Kuhn, H.G., Gage, F.H. (1997). More hippocampal neurons in adult mice living in an enriched environment. *Nature*, 386, 493-495.
- Kempermann, G., Kuhn, H.G., & Gage, F.H. (1998). Experience-induced neurogenesis in the senescent dentate gyrus. *The Journal of Neuroscience*, 18, 3206-3212.

- Kempermann, G., Jessberger, S., Steiner, B., & Kronenberg, G. (2004). Milestones of neuronal development in the adult hippocampus. *Trends in Neurosciences*, 27, 447-452.
- Komitova, M., & Eriksson, P.S. (2004). Sox-2 is expressed by neural progenitors and astroglia in the adult rat brain. *Neuroscience Letters*, 369, 24-27.
- Kronenberg, G., Reuter, K., Steiner, B., Brandt, M.D., Jessberger, S., Yamaguchi, M., & Kempermann G. (2003). Subpopulations of proliferating cells of the adult hippocampus respond differently to physiologic neurogenic stimuli. *The Journal of Comparative Neurology*, 467, 455-463.
- Kronenberg, G., Bick-Sander, A., Bunk, E., Wolf, C., Ehninger, D., & Kempermann, G. (2006). Physical exercise prevents age-related decline in precursor cell activity in the mouse dentate gyrus. *Neurobiology of Aging*, 27, 1505-1513.
- Kuhn, H.G., Dickinson-Anson, H., & Gage, F.H. (1996). Neurogenesis in the dentate gyrus of the adult rat: age-related decrease of neuronal progenitor proliferation. *The Journal of Neuroscience*, 16, 2027-2033.
- Kuhn, H.G., Winkler, J., Kempermann, G., Thal, L.J., & Gage, F.H. (1997). Epidermal growth factor and fibroblast growth factor-2 have different effects on neural progenitors in the adult rat brain. *The Journal of Neuroscience*, 17, 5820-5829.
- Kwak, S., & Matus, A. (1988). Denervation induces long-lasting changes in the distribution of microtubule proteins in hippocampal neurons. *Journal of Neurocytology*, 17, 189-195.

- Lagace, D.C., Yee, J.K., Bolanos, C.A., & Eisch A.J. (2006). Juvenile administration of methylphenidate attenuates adult hippocampal neurogenesis. *Biological Psychiatry*, *60*, 1121-1130.
- Lagace, D.C., Whitman, M.C., Noonan, M.A., Ables, J.L., DeCarolis, N.A., Arguello, A.A., Donovan, M.H., Fischer, S.J., Farnbauch, L.A., Beech, R.D., DiLeone, R.J., Greer, C.A., Mandyam, C.D., & Eisch, A.J. (2007). Dynamic contribution of nestin-expressing stem cells to adult neurogenesis. *The Journal of Neuroscience*, *27*, 12623-12629.
- Lichtenwalner, R.J., Forbes, M.E., Bennett, S.A., Lynch, C.D., Sonntag, W.E., & Riddle, D.R. (2001). Intracerebroventricular infusion of insulin-like growth factor-I ameliorates the age-related decline in hippocampal neurogenesis. *Neuroscience*, *107*, 603-613.
- Lim, D.A., Huang, Y.C., & Alvarez-Buylla, A. (2007). The adult neural stem cell niche: lessons for future neural cell replacement strategies. *Neurosurgery Clinics of North America*, *18*, 81-92.
- Liu, X., Wang, Q., Haydar, T.F., & Bordey, A. (2005). Nonsynaptic GABA signaling in postnatal subventricular zone controls proliferation of GFAP-expressing progenitors. *Nature Neuroscience*, *8*, 1179-1187.
- Mandyam, C.D., Harburg, G.C., & Eisch, A.J. (2007). Determination of key aspects of precursor cell proliferation, cell cycle length and kinetics in the adult mouse subgranular zone. *Neuroscience*, *146*, 108-122.

- Melvin, N.R., Poda, D., & Sutherland, R.J. (2007a). A simple and efficient alternative to implementing systematic random sampling in stereological designs without a motorized microscope stage. *Journal of Microscopy*, 228, 103-106.
- Melvin, N.R., Spanswick, S.C, Lehmann, H., & Sutherland, R.J. (2007b). Differential neurogenesis in the adult rat dentate gyrus: an identifiable zone that consistently lacks neurogenesis. *The European Journal of Neuroscience*, 25, 1023-1029.
- Mignone, J.L., Kukekov, V., Chiang, A.S., Steindler, D., & Enikolopov, G. (2004). Neural stem and progenitor cells in nestin-GFP transgenic mice. *The Journal of Comparative Neurology*, 469, 311-324.
- Mohedano-Moriano, A., Martinez-Marcos, A., Pro-Sistiaga, P., Blaizot, X., Arroyo-Jimenez, M.M., Marcos, P., Artacho-Perula, E., & Insausti R. (2008). Convergence of unimodal and polymodal sensory input to the entorhinal cortex in the fascicularis monkey. *Neuroscience*, 151, 255-271.
- Monfils, M.H., Driscoll, I., Melvin, N.R., & Kolb, B. (2006). Differential expression of basic fibroblast growth factor-2 in the developing rat brain. *Neuroscience*, 141, 213-221.
- Morshead, C.M., Reynolds, B.A., Craig, C.G., McBurney, M.W., Staines, W.A., Morassutti, D., Weiss, S., van der Kooy, D. (1994). Neural stem cells in the adult mammalian forebrain: a relatively quiescent subpopulation of subependymal cells. *Neuron*, 13, 1071-1082.
- Mouton, P. (2002). *Principles and practices of unbiased stereology*. Baltimore, MD: The Johns Hopkins University Press.

- Nacher, J., Alonso-Llosa, G., Rosell, D.R., McEwen, B.S. (2003). NMDA receptor antagonist treatment increases the production of new neurons in the aged rat hippocampus. *Neurobiology of Aging*, 24, 273-284.
- Namba, T., Mochizuki, H., Onodera, M., Mizuno, Y., Namiki, H., & Seki, T. (2005). The fate of neural progenitor cells expressing astrocytic and radial glial markers in the postnatal rat dentate gyrus. *The European Journal of Neuroscience*, 22, 1928-1941.
- Nern, C., & Momma, S. (2006). The realised niche of adult neural stem cells. *Stem Cell Reviews*, 2, 233-240.
- Nilsson, M., Perfilieva, E., Johansson, U., Orwar, O., & Eriksson, P.S. (1999). Enriched environment increases neurogenesis in the adult rat dentate gyrus and improves spatial memory. *The Journal of Neurobiology*, 39, 569-578.
- Nyengaard, J.R. (1999). Stereologic methods and their application in kidney research. *Journal of the American Society of Nephrology*, 10, 1100-1123.
- Olson, A.K., Eadie, B.D., Ernst, C., & Christie, B.R. (2006). Environmental enrichment and voluntary exercise massively increase neurogenesis in the adult hippocampus via dissociable pathways. *Hippocampus*, 16, 250-260.
- Palmer, T.D., Takahashi, J., & Gage, F.H. (1997). The adult rat hippocampus contains primordial neural stem cells. *Molecular and Cellular Neurosciences*, 8, 389-404.
- Palmer, T.D., Willhoite, A.R., & Gage, F.H. (2000). Vascular niche for adult hippocampal neurogenesis. *The Journal of Comparative Neurology*, 425, 479-494.

- Paxinos, G., & Watson, C. (1998). *The rat brain in stereotaxic coordinates* (4th ed.). San Diego, CA: Academic Press.
- Primrose, S.B., & Twyman, R.M. (2006). *Principles of gene manipulation and genomics* (7th ed.). Malden, MA: Blackwell Publishing.
- Rai, K.S., Hattiangady, B., & Shetty, A.K. (2007). Enhanced production and dendritic growth of new dentate granule cells in the middle-aged hippocampus following intracerebroventricular FGF-2 infusions. *The European Journal of Neuroscience*, *26*, 1765-1779.
- Rao, M.S., & Shetty, A.K. (2004). Efficacy of doublecortin as a marker to analyse the absolute number and dendritic growth of newly generated neurons in the adult dentate gyrus. *The European Journal of Neuroscience*, *19*, 234-246.
- Rao, M.S., Hattiangady, B., & Shetty, A.K. (2006). The window and mechanisms of major age-related decline in the production of new neurons within the dentate gyrus of the hippocampus. *Aging Cell*, *5*, 545-558.
- Reynolds, B.A., & Weiss, S. (1992). Generation of neurons and astrocytes from isolated cells of the adult mammalian central nervous system. *Science*, *255*, 1707-1710.
- Rhodes, J.S., van Praag, H., Jeffrey, S., Girard, I., Mitchell, G.S., Garland, T. Jr., & Gage F.H. (2003). Exercise increases hippocampal neurogenesis to high levels but does not improve spatial learning in mice bred for increased voluntary wheel running. *Behavioral Neuroscience*, *118*, 1006-1016.
- Richards, L.J., Kilpatrick, T.J., & Bartlett, P.F. (1992). De novo generation of neuronal cells from the adult mouse brain. *Proceedings of the National Academy of Sciences of the United States of America*, *89*, 8591-8595.

- Sahay, A., & Hen, R. (2007). Adult hippocampal neurogenesis in depression. *Nature Neuroscience, 10*, 1110-1115.
- Sapolsky, R.M. (1992). Do glucocorticoid concentrations rise with age in the rat? *Neurobiology of Ageing, 13*, 171-174.
- Schmidt-Hieber, C., Jonas, P., & Bischofberger, J. (2004). Enhanced synaptic plasticity in newly generated granule cells of the adult hippocampus. *Nature, 429*, 184-187.
- Schmitz, C., & Hof, P.R. (2000). Recommendations for straightforward and rigorous methods of counting neurons based on a computer simulation approach. *Journal of Chemical Neuroanatomy, 20*, 93-114.
- Schmitz, C., & Hof, P.R. (2005). Design-based stereology in neuroscience. *Neuroscience, 130*, 813-831.
- Schobersberger, W., Hobisch-Hagen, P., Fries, D., Wiedermann, F., Rieder-Scharinger, J., Villiger, B., Frey, W., Herold, M., Fuchs, D., & Jelkmann, W. (2000). Increase in immune activation, vascular endothelial growth factor and erythropoietin after an ultramarathon run at moderate altitude. *Immunobiology, 201*, 611-620.
- Seaberg, R.M., & van der Kooy, D. (2002). Adult rodent neurogenic regions: the ventricular subependyma contains neural stem cells, but the dentate gyrus contains restricted progenitors. *The Journal of Neuroscience, 22*, 1784-1793.
- Segovia, G., Yague, A.G., Garcia-Verdugo, J.M., & Mora, F. (2006). Environmental enrichment promotes neurogenesis and changes the extracellular concentrations of glutamate and GABA in the hippocampus of aged rats. *Brain Research Bulletin, 70*, 8-14.

- Seri, B., Garcia-Verdugo, J.M., McEwen, B.S., & Alvarez-Buylla, A. (2001). Astrocytes give rise to new neurons in the adult mammalian hippocampus. *The Journal of Neuroscience*, *21*, 7153-7160.
- Seri, B., Garcia-Verdugo, J.M., Collado-Morente, L., McEwen, B.S., & Alvarez-Buylla, A. (2004). Cell types, lineage, and architecture of the germinal zone in the adult dentate gyrus. *The Journal of Comparative Neurology*, *478*, 359-378.
- Shapiro, L.A., Upadhyaya, P., & Ribak, C.E. (2007). Spatiotemporal profile of dendritic outgrowth from newly born granule cells in the adult rat dentate gyrus. *Brain Research*, *1149*, 30-37.
- Shen, Q., Goderie, S.K., Jin, L., Karanth, N., Sun, Y., Abramova, N., Vincent, P., Pumiglia, K., & Temple, S. (2004). Endothelial cells stimulate self-renewal and expand neurogenesis of neural stem cells. *Science*, *304*, 1338-1340.
- Shetty, A.K., Hattiangady, B., & Shetty, G.A. (2005). Stem/progenitor cell proliferation factors FGF-2, IGF-1, and VEGF exhibit early decline during the course of aging in the hippocampus: role of astrocytes. *Glia*, *51*, 173-186.
- Shihabuddin, L.S., Horner, P.J., Ray, J., & Gage, F.H. (2000). Adult spinal cord stem cells generate neurons after transplantation in the adult dentate gyrus. *The Journal of Neuroscience*, *20*, 8727-8735.
- Shors, T.J., Townsend, D.A., Zhao, M., Kozorovitskiy, Y., & Gould, E. (2002). Neurogenesis may relate to some but not all types of hippocampal-dependent learning. *Hippocampus*, *12*, 578-584.

- Singh, R., Maganti, R.J., Jabba, S.V., Wang, M., Deng, G., Heath, J.D., Kurn, N., & Wangemann, P. (2004). Microarray-based comparison of three amplification methods for nanogram amounts of total RNA. *American Journal of Physiology, Cell Physiology*. 288, C1179-1189.
- Slomianka, L., & West, M.J. (2005). Estimators of the precision of stereological estimates: an example based on the CA1 pyramidal cell layer of rats. *Neuroscience*, 136, 757-767.
- Snyder, J.S., Hong, N.S., McDonald, R.J., & Wojtowicz, J.M. (2005). A role for adult neurogenesis in spatial long-term memory. *Neuroscience*, 130, 843-852.
- Steindler, D.A. (2007). Stem cells, regenerative medicine, and animal models of disease. *Institute of Laboratory Animal Resources Journal*, 48, 323-338.
- Suh, H., Consiglio, A., Ray, J., Sawai, T., D'Amour, K.A., & Gage, F.H. (2008). In Vivo Fate Analysis Reveals the Multipotent and Self-Renewal Capacities of Sox2(+) Neural Stem Cells in the Adult Hippocampus. *Cell Stem Cell*, 1, 515-528.
- Tanaka, T., Koizumi, H., & Gleeson, J.G. (2006). The doublecortin and doublecortin-like kinase 1 genes cooperate in murine hippocampal development. *Cerebral Cortex*, 16, 69-73.
- Tang, Y., Nyengaard, J.R., Pakkenberg, B., & Gundersen, H.J.G. (2003). Stereology of neuronal connections (myelinated fibres of white matter and synapses of neocortex) in human brain. *Image Analysis and Stereology*, 22, 171-182.
- Tozuka, Y., Fukuda, S., Namba, T., Seki, T., & Hisatsune, T. (2005). GABAergic excitation promotes neuronal differentiation in adult hippocampal progenitor cells. *Neuron*, 47, 803-815.

- Trejo, J.L., Carro, E., & Torres-Aleman, I. (2001). Circulating insulin-like growth factor I mediates exercise-induced increases in the number of new neurons in the adult hippocampus. *The Journal of Neuroscience*, *21*, 1628-1634.
- Urbanska, E.M., Czuczwar, S.J., Kleinrok, Z., & Turski, W.A. (1998). Excitatory amino acids in epilepsy. *Restorative Neurology and Neuroscience*, *13*, 25-39.
- van Praag, H., Kempermann, G., & Gage, F.H. (1999). Running increases cell proliferation and neurogenesis in the adult mouse dentate gyrus. *Nature Neuroscience*, *2*, 266-270.
- van Praag, H., Schinder, A.F., Christie, B.R., Toni, N., Palmer, T.D., & Gage, F.H. (2002). Functional neurogenesis in the adult hippocampus. *Nature*, *415*, 1030-1034.
- Wagner, J.P., Black, I.B., & DiCicco-Bloom E. (1999). Stimulation of neonatal and adult brain neurogenesis by subcutaneous injection of basic fibroblast growth factor. *The Journal of Neuroscience*, *19*, 6006-6016.
- Wang, S., Scott, B.W., & Wojtowicz, J.M. (2000). Heterogenous properties of dentate granule neurons in the adult rat. *Journal of Neurobiology*, *42*, 248-257.
- Wegner, M., & Stolt, C.C. (2005). From stem cells to neurons and glia: a Soxist's view of neural development. *Trends in Neurosciences*, *28*, 583-588.
- Weissman, I.L. (2000). Stem cells: units of development, units of regeneration, and units in evolution. *Cell*, *100*, 157-168.
- Wennstrom, M., Hellsten, J., Ekdahl, C.T., & Tingstrom, A. (2003). Electroconvulsive seizures induce proliferation of NG2-expressing glial cells in adult rat hippocampus. *Biological Psychiatry*, *54*, 1015-1024.

- West, M.J., Slomianka, L., & Gundersen, H.J. (1991). Unbiased stereological estimation of the total number of neurons in the subdivisions of the rat hippocampus using the optical fractionator. *The Anatomical Record*, 231, 482-497.
- Weston, A.D., & Hood, L. (2004). Systems biology, proteomics, and the future of health care: toward predictive, preventative, and personalized medicine. *Journal of Proteome Research*, 3, 179-196.
- Xie, T., & Spradling, A.C. (2000). A niche maintaining germ line stem cells in the Drosophila ovary. *Science*, 290, 328-330.
- Yen, T.H., & Wright, N.A. (2006). The gastrointestinal tract stem cell niche. *Stem Cell Reviews*, 2, 203-212.
- Yeoh, J.S., & de Haan, G. (2007). Fibroblast growth factors as regulators of stem cell self-renewal and aging. *Mechanisms of Ageing and Development*, 128, 17-24.
- Zaman, V., & Shetty, A.K. (2003). Pretreatment of donor cells with FGF-2 enhances survival of fetal hippocampal CA3 cell transplants in the chronically lesioned young adult hippocampus. *Experimental Neurology*, 183, 11-24.
- Zheng, W., Nowakowski, R.S., & Vaccarino, F.M. (2004). Fibroblast growth factor 2 is required for maintaining the neural stem cell pool in the mouse brain subventricular zone. *Developmental Neuroscience*, 26, 181-196.